Effect of Convergent Absorber Tube on Performance of Nanofluid Based Parabolic Trough Collector

A dissertation submitted in partial fulfilment of requirement for the award of degree of

Master of Engineering

in

Thermal Engineering

Submitted by

ANUJ BABBAR

Roll No.: 801583004

Under the guidance of

Mr. KUNDAN LAL RANA

Assistant Professor

DEPARTMENT OF MECHANICAL ENGINEERING

THAPAR UNIVERSITY

PATIALA (PB), INDIA, 147004

July, 2017

CERTIFICATE

I hereby declare that the work done in this thesis entitled "**Effect of Convergent Absorber Tube on Performance of Nanofluid Based Parabolic Trough Collector.**" submitted towards partial fulfilment of requirement for award of degree of **Master of Engineering** in **Thermal Engineering, Thapar University, Patiala,** is an authentic record of the work carried out by me under the supervision and guidance of **Mr. Kundan Lal Rana, Assistant Professor, Mechanical Engineering Department, Thapar University, Patiala.**

The matter embodied in this report has not been submitted in part or full to any other university or institute for the award of any degree.

Dated: 17th July 2017

Anuj babbar

Roll No.: 801583004

This is to certify that above declaration made by the student concerned is correct to the best of our knowledge and belief.

.....

Mr. Kundan Lal Rana

Assistant Professor

Mechanical Engineering Department

Thapar University, Patiala

ACKNOWLEDGEMENT

I would like to express my deepest sense of gratitude and a very sincere thanks to my guide **Mr. Kundan Lal Rana**, Assistant Professor, Mechanical Engineering Department, Thapar University, Patiala for his sincere and invaluable guidance and full support which helped me in the accomplishment of this seminar report in present form. His dynamic and diligent enthusiasm has been highly instrumental in keeping my spirits high. His flawless and forthright suggestions blended with an innate intelligent application have crowned my task with success.

Anuj Babbar

Roll No. : 801583004

Abstract

Solar collector is one of the efficient devices to utilize the solar energy. To trap maximum solar energy, a lot of changes and approximations have been done in conventional solar heat collectors. In which one of the method is by changing working fluid that can absorb maximum solar energy. Nanofluid plays a major role in heat transfer field. In this proposed thesis work, an attempt has been made to enhance the performance of solar collector, by changing the geometry of absorber tube. An experimental investigation is done on parabolic trough collector, having a convergent absorber tube and making use of nanofluid as working fluid. Experiments were conducted in convergent and straight absorber tube (inlet diameter is 31 mm and outlet diameter is 12.7 mm). Two different working fluids were used, distilled water andAl_2O_3-H_2O nanofluid of different volumetric concentration 0.01%, 0.045% and 0.08% of, at 150LPH, 200LPH, and 250LPH mass flow rates. To investigate the performance of solar heat collector, heat gain by working fluid, instantaneous efficiency, and thermal efficiency were evaluated. It was observed that instantaneous efficiency of convergent absorber tube is slightly more (5% to 10%) than that of straight absorber tube for Al_2O_3–H_2O nanofluids of 0.01% and 0.045% volumetric concentration at 150LPH and 200LPH mass flow rates. It was also observed that with increase in mass flow rate instantaneous efficiency increases from 65% to 78%, as mass flow rate increases from 150 LPH to 250 LPH. Some of the thermophysical properties such as; thermal conductivity, viscosity, density, and pH were also analyzed, as they play important role to determine the efficiency of PTC. It was noticed that ratio of thermal conductivity of Al_2O_3-H_2O nanofluids to the base fluid increases with rise in temperature. Whereas, with time viscosity and density of Al_2O_3-H_2O nanofluids decreases with time i.e. viscosity vary from 5 % to 9 % and density decreases from 3% to 7%.

Keywords: Solar energy, convergent absorber tube, thermal conductivity, nanofluid, PTC.

Table of Contents

List of Figures

List of Tables

NOMENCLATURE

A_{aper}: Aperture area of collector m^2

C_p: Specific heat J/kg k

$C_{p,nf}$: Specific heat of nanofluid

$C_{p,np}$: Specific heat of nanoparticle

$C_{p,bf}$: Specific heat of basefluid

F_R : Heat removal factor

fv: Concentration by volume

G_t: Global solar intensity in W/m^2

k_{eff} : Effective thermal conductivity of suspension in W/m k

k_{bf} : Thermal conductivity of base fluid in W/m k

$K_{nf:}$ Thermal conductivity of nanofluid

$K_{np:}$ Thermal conductivity of nanoparticle

L: Length of collector in m

$\dot{m}$: Mass flow rate in kg/s

T_{in}: Teamperature at the inlet of absorber tube ($^{\cdot o}C$)

T_{out}: Temperature at the outlet of absorber tube ($^{\cdot o}C$)

V_{np}: Volume of nanoparticles in m^3

V_{bf}: Volume of base fluid in m^3

W: Width collector in m

W_{np}: Weight of nano-particles

qu : Rate of useful energy gained in W

$\tau\alpha$: Absorptance-transmittance product

$\alpha =$ k_s/k_{BF}

ψ: Spherecity

ρ_{np}: Density of nanoparticles

η_i: Instantaneous efficiency

η_t: Thermal efficiency

μ_{nf}: Dynamic viscosity of nanofluid

μ_{bf}: Dynamic viscosity of base fluid

Chapter 1

Introduction

1.1 Introduction

Energy is one of the most important driving force for the development of a nation and in order to fulfill the energy demand fossil fuels like coal; petroleum etc are mainly used as energy source. As per review, 76 million barrels of oil is consumed across the worldwide daily [1]. Usage of these fossil fuels leads to major problem like pollution, global warming etc due to harmful byproduct i.e. CO_2, CO etc released by their combustion. So in order to tackle both the problems i.e. increasing energy demand and pollution, one has to move towards renewable resources of energy. There are various type of renewable energy resources such as wind energy, solar energy, tidal energy. Among all the renewable sources of energy available like wind, solar, tidal, ocean thermal, solar thermal energy is the most plentiful source and is available in both direct as well as indirect forms. Hence, solar energy the best option for renewable source. By using of solar energy we can also achieve the concept of sustainable development. Though the solar energy is being used from primitive time but it has generated special interest today due to rise in pollution or environmental problem, and most of the countries are committed for research in this area to develop the sustainable source of energy.

1.2 Solar Heat Collector

It is like heat exchanger, which converts solar radiation into thermal energy. The major component of any solar system is a solar collector or concentrator. Solar collectors, an important component of any solar devices, absorb/focus the radiation incoming from the sun and transfer the heat to a transporting material like oil, water and air as internal energy. The absorber can take a variety of configurations. Solar heat collector can be classified broadly in two types

a) Non concentrator collector
b) Concentrator collector

1.2.1. Non concentrator collector

a) Flat plate solar heat collector

A flat plate collector is a low temperature collector i.e. used for low temperature applications. It consist of

- flat-plate absorber
- transparent cover that reduces heat losses
- heat-transport fluid to remove heat from the absorber
- heat insulating backing.

Solar radiation falls on it, passes through transparent cover and impinges on the absorber surface and a large amount of energy is absorbed by absorber surface and then this energy is transferred to the working fluid flowing in the tubes. A flat plate collector is shown in Figure 1.1.

Figure1.1: Flat plate solar heat collector. [2]

1.2.2 Concentrator collector

Following are the main types of concentrating type of collector

a) Parabolic trough collector (PTC)

In it solar radiations concentrated on absorber tube i.e. with the help reflecting surface, which focus solar radiations falling on it to the absorber tube. Absorber tube get heated and that heat is transferred to the working fluid flowing through it. A tracking device is attached to it, with the help of it, reflecting surface track sun i.e. it tracks the sun position so as to maintain focus of solar radiation on absorber tube.

b) Solar Bowl Heat Collector

A solar bowl is similar to parabolic trough collector but has a fixed mirror instead of a tracking mirror which a parabolic dish would use. A Solar Bowl heat collector is shown in Figure 1.2

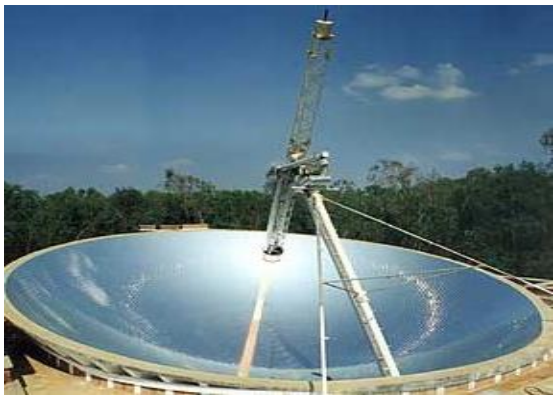

Figure 1.2: Bowl solar heat collector [3].

c) Heliostat

In a large array of reflecting surfaces usually plain mirror focus on a single point (solar tower). It is used in solar-thermal power plant i.e. solar radiation is focused on solar tower by array of plain mirrors and the fluid in it got so much heated and that hot fluid is used to generate steam for power generation.

1.3 Nanofluids

Nanofluids are two phase fluids where solid nanoparticles are suspended into basefluids. The key idea is to improve the efficiency of a system. The main application of nanofluids is in heat transfer applications such as; heat exchangers, solar heat collectors etc. Nanofluids are used in because they increase the thermal conductivity of the base fluid to enhance the heat transfer rate.

1.4 Nanofluids Preparation Methods

Preparation of nanofluids is very important to be known about the thermophysical properties of naofluids since particle agglomeration depends on preparation method of naofluid [4]. There are generally two techniques used to prepare nanofluids

A) Single step method

B) Two step method.

A) In single step method [5,6] the nanoparticles are dispersed directly into a base fluid. This method suits best for metallic nanofluids like copper, aluminum.

   In this technique the processes such as drying, storage, transportation, and dispersion of nanoparticles are avoided, so that the agglomeration of nanoparticles is minimized to some extent and the stability of fluids is increased

B) In two step method [7,8] nanoparticles are initially prepared and then dispersed into the fluid by some technique like shear [9], and ultrasound [10]. In other words, the two step technique uses physical or chemical processes to produce nanoparticle and proceeds to disperse them into a base fluid. Widely, two step method is used for the preparation of nanofluids.

Nanofluids can be prepared with surfactant or without surfactant. Role of surfactant is to disperse the nano particles in the base fluid, so that nanoparticles don't settle down easily. Some of the surfactant used by the researchers: Triton X-100, SDS (sodium dodeclysulfonate).

Figure 1.3: Al_2O_3 naonofluid solution a) without surfactant b) with surfactant.

1.4 Nanofluid applications

Now a days a lot of research is going on the scope of nanofluids applications in different fields i.e. mainly in heat transfer. Followings are the few area of in which nanofluids can be used or research is going on how efficiently nanofluids in these fields are:

- HEAT TRANSFER

- Heat exchangers
- For cooling in nuclear reactor
- Solar heat collector
- Cooling of diesel electric generator
- Solar water heating applications
- Application in transformer
- Space, defense and ships
- Refrigeration

- AUTOMOBILE
- As coolant
- In brakes

- Biomedical
- Cancer therapy
- Nono-drugs delivery

Chapter 2

Literature Review

2.1 General

In this chapter, the literature survey of different authors has been done whose work is related to solar heat collector, nanofluid based solar heat collector and on nanofluids. This chapter also includes literature review of the authors who had done parametric analysis of solar heat collector.

2.2 Review of Literature.

Jiang Y *et al.* (2016) investigated the conventional flat plate collector for water heating system in the cold places and found, it is less efficient because of low efficiency, large heat loss, tube burst and freeze. To overcome these problems a small sized parabolic trough collector is developed for the water heating at cold places. The experimental setup was developed under the condition of cold place to observe the characteristics of PTC. Results show the efficiency of collector was 67% when the solar radiation is less than 310 W/m^2. This indicate that the collector collect the radiation efficiently. From the results it was observed that with increase in the Reynolds number thermophysical properties of HTF can be improved and the efficiency of PTC is improved with the rise in temperature of the working fluid till temperature reaches 1000^oC [11].

Manikandan *et al.*(2012) did parametric analysis of a parabolic trough collector. The various parameters were chosen for the study such as; mass flow rate of the heat transfer fluid, different heat transfer fluid, solar insulation and concentration ratio. It was observed that rise in inlet temperature of the heat transfer fluid causes a decreasein efficiency of PTC, this was due to an increase in convective and radiation losses to the surroundings. The water and castor oil were used as the heat transfer fluids for comparison. It was alsoobserved that the effective heat gain was more with water than with castor oil. This was due to the fact that water was having more specific heat than castor oil. It was also observed that the effective heat gain increases with an increase in intensity of sun rays [12].

Zhang H *et al.* (2015) compared numerically 1-D and 3-D model results with the experimentally setup results, exited at the Sandia National Laboratory. From the results, it was observed that difference of the temperature at the output of a receiver tube is 0.65^0C in the case of 1-D model. But in the case of 3-D model the difference of temperature is about 2.69^0C. So, from the results we can say that the 1-D model gives better results as compare to the 3-D model. Assumption for the 1-D model is, convective heat transfer between the glass and tube annulus, conduction through glass cover, absorber and support brackets; radiation in the annulus and from the glass to the sky. Assumptions in the case of 3-D model are more as compare to the 1-D model. Hence, error is large in the case of 3-D model [29].

Anton J M *et al.* (2014) experimented investigated by using the gas in the PTC as a heat transfer fluid. It has good advantages as compare to the use of oil. A testing setup was built to check the technically feasibility of the new technology. In the case of oil there is limitation of a temperature range but in the case of gas temperature range is very high. Due to this thermal efficiency of system increases and very high working pressure reduce the pumping power[25].

Ernani Favale *et al.* (2012) had investigated diathermic oil based nanofluids. In order to reduce the construction cost and high level safety guarantee of the system, diathermic oil was used as heat transfer fluid in many applications especially, when high temperatures and low pressure are required. They studied the change in thermal conductivity of different nanofluid with change in volumetric concentration as shown in Figure 2.1 [13].

To predict the thermal conductivity of solid-liquid mixtures researcher has gave there models like Hamilton and Crosser [28].

$$\frac{K_{eff}}{K_{bf}} = \frac{\alpha+(n-1)-(n-1)(1-\alpha)\upsilon}{\alpha+(n-1)+(1-\alpha)\upsilon} \qquad (2.1)$$

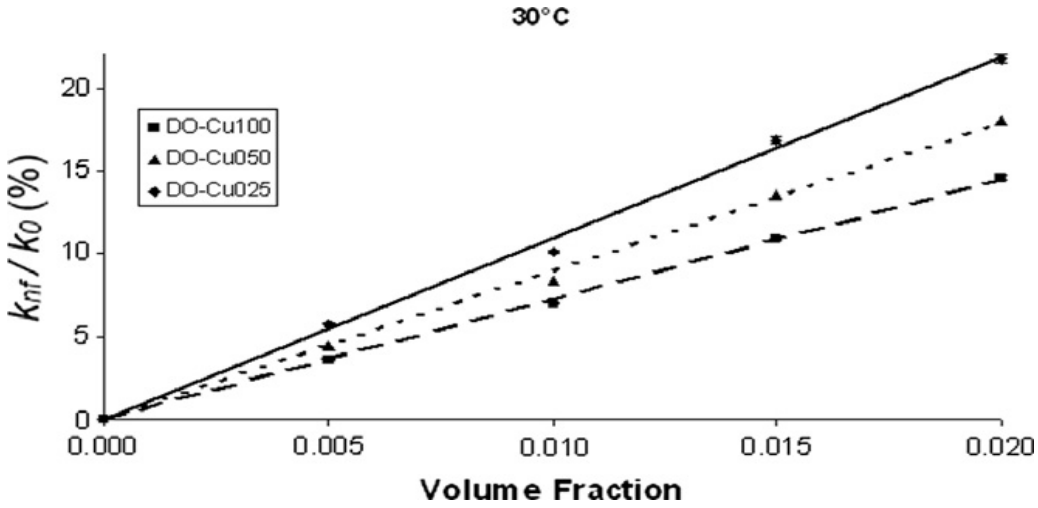

Figure 2.1: Experimental data for nanofluids with oil and CuO nanoparticles with different particle sizes [13].

They found that thermal conductivity of nanofluid is directly proportional to the volume fraction, particle size of nanoparticles, and which could influence the heat transfer mechanisms, temperature does not influence the thermal conductivity enhancement of the nanofluids. They found that Hamilton–Crosser model undervalues the experimental data, so nanofluids thermal conductivity depends on other heat transfer mechanisms which are not considered in this model[13].

Cheng *et al*. (2014) had performed a large number of experiments, on sensitivity analysis and design optimization of a parabolic trough collector. Six different parabolic trough collector named as LS-2, LS-3, Sky Trough, Euro Trough, LAT 73, Helio Trough and Ultimate Trough along with four different receiver tube named as LS-2 receiver, LS-3 receiver, Siemens UVAC 2010 receiver and Schott PTR 70 receiver were used. From the results it was found that UVAC 2010 receiver absorb large amount of heat energy and the LAT 73 has the best optical efficiency as compare to other collector [30].

Farzad Veysi *et al.* (2011) had investigated the effect of Al_2O_3-H_2O nanofluids with surfactant Triton X-100 on efficiency of flat-plate solar collectors. The spherical shaped Al_2O_3 powder was having an average diameter of 15nm. ASHRAE standards 86-93 were used in calculating the efficiency of flat-plate collector [14]. By knowing all the temperatures, useful energy can be calculated as;

$$Q_u = mC_p(T_o - T_i) \quad (2.2)$$

$$Q_u = A_c F_R[G_T(\tau\alpha) - U_L(T_i - T_a)] \quad (2.3)$$

They found that by using 0.2 wt% of Al_2O_3-H_2O nanofluid, efficiency of solar collector was increased by 28.3% as compared to D.I. water used as working [15].

FarzadVeisy*et al*. (2012) had conducted the same experiment as conducted by Farzad Veysiet al. (2011) and by same methodology by using MWCNT-H_2O with tow concentration i.e. 0.2wt% and 0.4%. They found that by using surfactant with 0.2 wt% of MWCNT nanofluid increases the efficiency as compare to nanofluid used without surfactant. Whereas, using surfactant for 0.4 wt% MWCNT nanofluid efficiency decreases as compare to MWCNT nanofluids without surfactant [16].

Padilla *et al.(2014)* performed the exergy analysis on a parabolic trough solar receiver. The purpose of the study was to know the effects of various environmental and operational parameters on the performance of the parabolic trough collectors. Different parameters whose effect was to be seen on the performance, were mass flow rate of heat transfer fluid, inlet temperature, pressure in annulus, wind speed and solar intensity. The study was based on heat transfer models which have been used before by other authors. It was observed that vacuum in the annulus between the glass and the tube along with the intensity of solar radiation have a significant effects on thermal and exergetic performance of the collector whereas, other parameters were not affecting the performance significantly. Pressure less than 1 Torr is maintained in vacuum and solar intensity varied between 250 to 1000 W/m^2 [17].

M.H. SAJID *et al.* (2013) had experimentally investigated the thermophysical properties of nanofluids. They found that fluid having very small amount of nanoparticles have considerable higher thermal conductivity than that of basefluid. The viscosity of nanofluid is directly proportional to volume concentration of nanoparticles. Whereas for alumina nanofluids viscosity decreases exponentially with an increase in temperature. Hysteresis behavior was also observed for all the nanofluids in Figure 2.2. Variation in thermal conductivity with volume fraction of nanofluids of different concentration, which are prepared at different time is shown in Figure 2.3 [18].

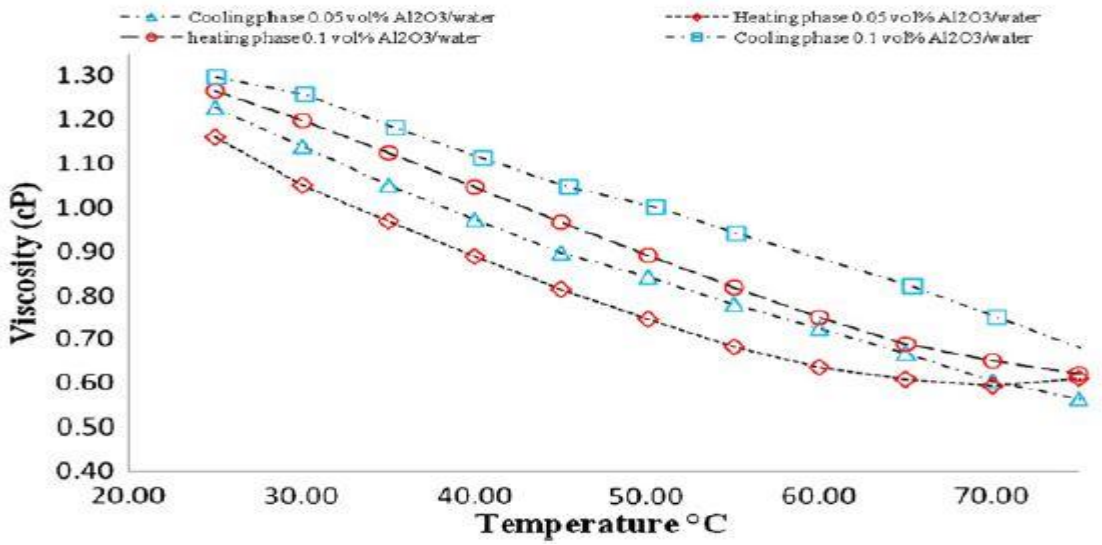

Figure 2.2: Hysteresis observed for Al2O3/water for 13 nm, particle volume fractions of 0.05 and 0.1%[18].

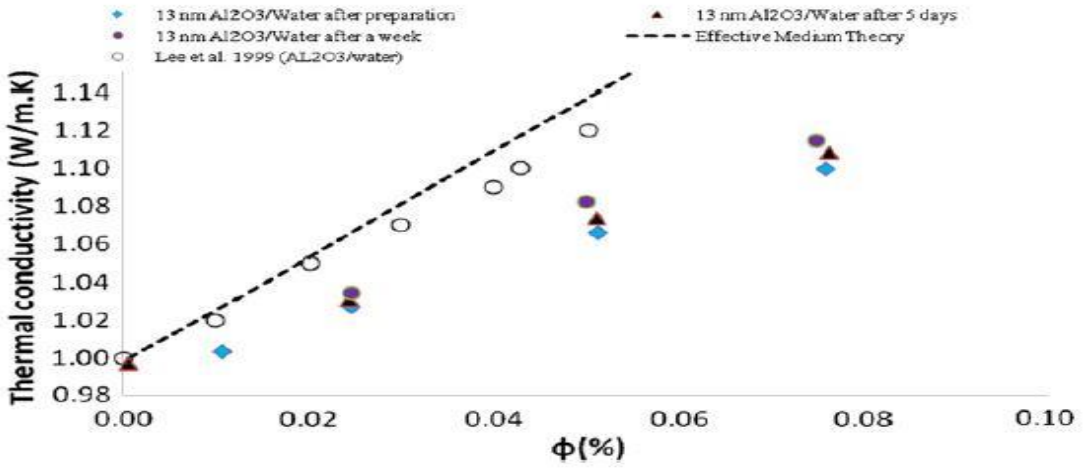

Figure2.3: Thermal conductivity of Al_2O_3/water nanofluids at different volume fractions at 25^oC [18].

Lupfert *et al.* (2008) experimentally investigated thermal properties of receivers of a parabolic trough. In this study different methods to calculate the thermal loss from a receiver tube were presented based on their operating temperature. Two different receiver tubes which are Solel UVAC and Schott PTR 70 were used for the purpose of experiment. A single receiver tube of 4m length was heated up using a 4m long quartz heating element which was placed inside the tubes. The temperature measurements were done using 14 thermocouple

placed accordingly at different places on the tube. It was observed that the solar parabolic trough plants which are having a temperature range of about 390^{o}C were having an energy loss of about 300W/m of receiver length [19].

F. Nejati *et al.* (2014) had investigated the effect of pH variation of nanofluid on thermal efficiency of solar collector with helical tube. They used nanofluids CuO-H_2O and Al_2O_3-H_2O with surfactant SDS (sodium do decly sulfonate). They found that the more the differences between the pH of nanofluid used and the iso-electric point pH of that naonofluid, more is the increase in the thermal efficiency of the solar collector. Al_2O_3 nanofluid (pH_{IEP} = 7.4) at the basic condition (pH = 10.5) the efficiency of the collector is calculated by 64.5% greater than that with the nanofluid at pH = 9.2 [20].

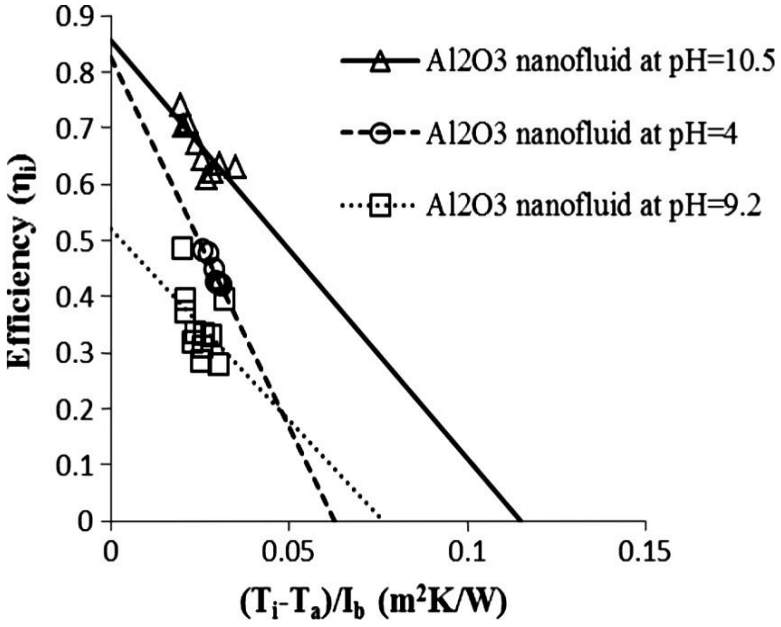

Figure 2.4: The efficiency of the cylindrical solar collector with Al2O3 nanofluid at three different pH values. [20]

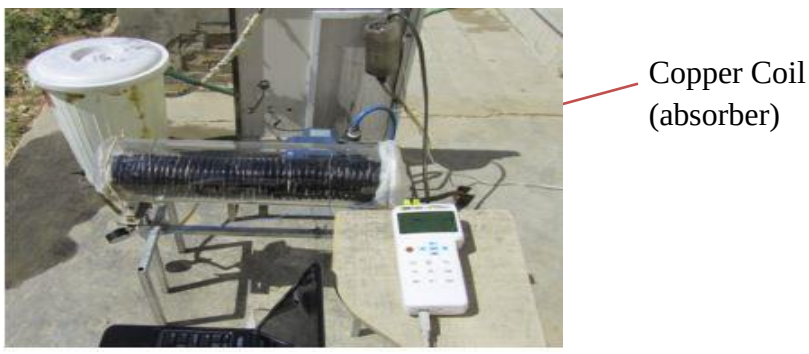

Figure 2.5: Experimental setup [20].

Larcher *et al.* (2014) had conducted the experiments to investigate the optical efficiency on the basis of optical behavior of collector at high and low temperature condition. Also the heat loss from the receiver tube when the temperature is high and no radiation. The efficiency is calculated for the operating temperature up to 200^0C and measurement was done determine the value of incidence angle modifier (IAM) [21].

Colangelo *et al.* (2013) has worked on transparent flat plate panel to reduce sedimentation of Al_2O_3 nanofluids. They had modified the flat plate panel and made bottom header and top header of varying cross-section in order to achieve constant mean velocity. They found that there is less precipitation as compare to conventional flat plate panel and concluded that the amount of deposited solid phase is inversely proportional to mean velocity and directly proportional to volume fraction of solid phase [22].

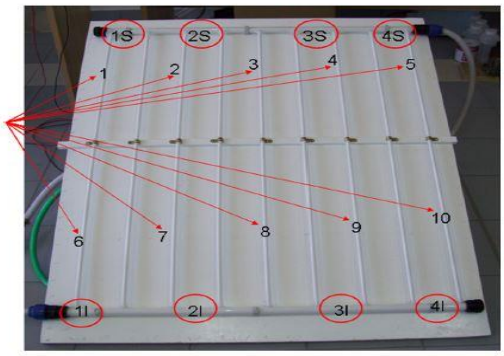

Figure2.6: Transparent flat plate panel [22].

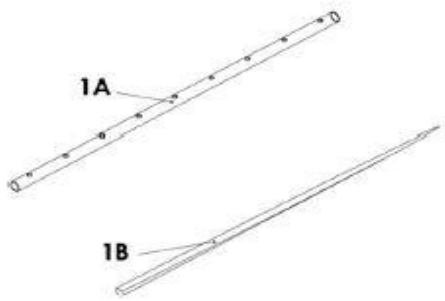

Figure 2.7:Modified header [22].

Y. Hwang *et al.*(2007) have done work on the stability and thermophysical properties of CuO-with water and ethylene-glycol, multi-walled carbon nanotube (MWCNT)-in oil and in water, silicon oxide in water etc nanofluids. They found that thermal conductivity enhancement of nanofluid strongly depends on the thermal conductivity of base fluid and found that CuO and MWCNT in oil has more thermal conductivity than that in water. They examined nanofluid with UV-vs spectrophotometer to estimate its stability. Moreover they also found that addition of sodium dodecly sufate (SUS) surfactant increases the stability of nanofluid [23].

A. Ghadimi *et al.* (2011) had discussed about sedimentation of nanoparticles. Things on which sedimentation of nanoparticles depends are surfactant or activator addition, ph of solution, ultrasonic vibration. By addition of surfactant and by controlling ph of nanofluid surface properties of suspended nanoparticles are changed and suppress the forming cluster of

particles, to attain stable suspension whereas in ultra sonic bath break down the agglomerations. To inspect the stability of nanofluid UV-Vis spectrophotometer, zeta potential test, Sediment photography capturing, TEM (Transmission Electron Microscopy) and Scanning Electron Microscope (SEM), Light scattering method, Sedimentation balance method, Three omega methods were used [24].

Bellos *et al.* (2016) used wavy absorber tube in order to increase inner surface area of absorber tube and to increase turbulence inside the absorber tube in order to increase the heat transfer coefficient. They conducted experiments by using thermal oil, oil nanofluids and pressurized water as working fluid and examined exergy efficiency, thermal efficiency, receiver temperature, thermal losses coefficient and heat transfer coefficient. They found that receiver tube temperature is more in case of oil nanofluid than that of pressurized water which results in lesser thermal efficiency for oil nanofluid, whereas exergy efficiency was more in case of oil nanofluid, as the specific heat for oil nanofluid is less than that of water. In it they also compared the results with cylindrical absorber tube and found that wavy absorber tube has more exergy efficiency and thermal efficiency than that of cylindrical absorber tube as heat transfer coefficient is more in case of wavy tube [26]. The inside geometry of wavy absorber tube is shown in Figure 2.9.

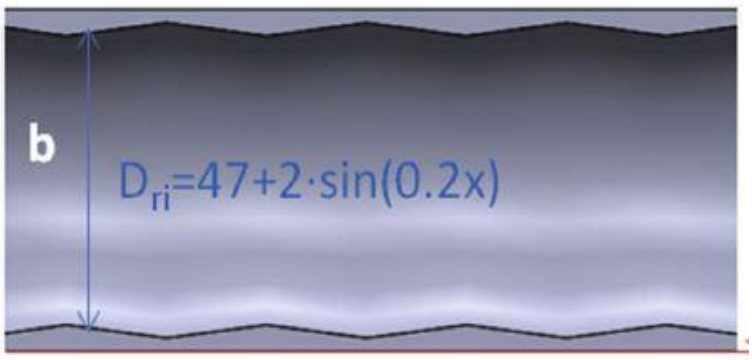

Figure2.8: Wavy Absorber Tube [26].

2.3 Gap Study and Objective

2.3.1 Gap study

A lot of research work is being done and is still going on the applications of nanofluid in solar heat collector. Many of the researchers are trying to improve the efficiency and effectiveness of solar heat collector by using different methods i.e by decreasing sedimentation, by addition of chemicals to change nanofluid ph value, by changing the shape

of absorber tube, by adding surfactant etc. While going through literature following points were observed.

- Nonofluids is the emerging field where they can be explored for their application in solar thermal area.
- A limited work has been reported in the application of nanofluids.
- The idea of using convergent absorber tube has been not much explored
- A very limited work has been reported on how to increase the stability of nanofluids by using different geometries of the absorber tubes.

2.3.2 Objectives

Following are the objectives

1. To investigate the performance of convergent absorber tube PTC.
2. To study the effect of convergent absorber tube on the thermophysical properties of nanofluid.
3. To compare the performance of convergent absorber tube and straight absorber tube PTC.

Chapter 3
Equipments and Experimental Methodology

3.1 Parabolic Trough Collector

A parabolic Trough collector (PTC) is made by bending the sheet of a reflecting material in the parabolic shape. Reflecting material may be a polished mirror, aluminum sheet, etc. In present work, reflecting surface is made by using polished stainless steel material due to its non-corrosive property and high reflectivity. Radiation from the sun falls on the trough parallel to its plane of symmetry. From the trough surface these radiation are reflected or concentrated to its focal line. A receiver tube is placed along the focal line of parabola. The receiver tube or the absorber tube is covered by the concentric glass cover tube to reduce the convective loss. The heat transfer fluid which is flowing through the absorber tube get heated to a high temperature. Sun is track in the east-west direction. Parabolic trough collector test rig is as shown in Figure 3.1.

Figure 3.1: Parabolic trough collector

3.2Components of Parabolic Trough Collector

The main component of PTC are listed below:

- Reflector
- Tracking system
- Heat absorber tube
- Storage tank
- Pump

3.2.1 Reflector

Reflecting surface is the most important component for the working of a parabolic trough collector. So, for the reflection the material which has the high reflectivity are used. In the present work reflector made up with the Stainless steel of reflectivity near to one. Dimension of the reflector given in the Table no. 3.1.

3.2.2 Tracking System

The collector is oriented in the North-South direction and tracks in the East-West direction by using the micro-controller. The main component of a tracking system is a stepper motor is shown in a Figure 3.2. Stepper motor is used to rotate the reflector for tracking the sun with minimum step size of 0.004^0. The advantage of this tracking mechanism is that the small adjustment is required during the start of the day of experiment. Span for track the sun is 40^0east to 40^0 west. Tracker is move accordance with the sun speed i.e. reflector cover 15^0 in one hour with the speed of Sun

Figure 3.2: Stepper Motor.

3.2.3 Absorber Tube

It is also known as the receiver of the PTC. It is placed along the focal line of a parabola. In absorber tube is the most important element of the system. Material of the absorber tube has good thermal properties. It has a good thermal conductivity, in the present case we are using two different absorber tubes both made up of copper, one tube is of converging geometry as

shown in Figure 3.3, inlet diameter of 0.0381 m and outlet diameter is 0.0127 m, and other tube is of constant diameter as shown in Figure 3.4, inner diameter of 0.0285 m, thickness of absorber tube is 0.0005 m. To increase the absorptive of the copper tube a thin film of black paint is used on it. Absorber tube is covered with the glass tube of the outer diameter 0.0504 m to reduce the convective heat loss from the receiver tube.

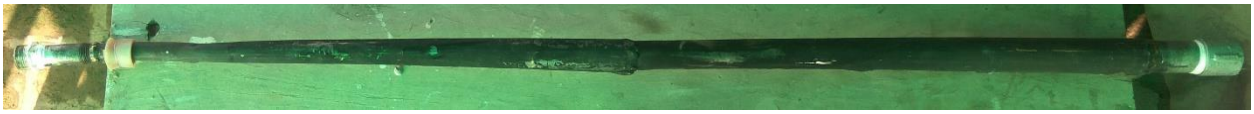

Figure 3.3: Convergent Absorber Tube.

Figure 3.4: Straight Absorber Tube.

3.3 Storage Tank

A storage tank is a type of container made up of Galvanized iron sheet having 12 litres capacity filled with water or nanofluid used as a working fluid. The water/nanofluid is circulated from the container with the help of a pump to the inlet of the receiver tube. Water/nanofluid after gaining heat from the receiver tube is dropped in the same container and is re-circulated again with the help of a pump. The GI tank is double insulated with 2 mm and 4 mm thick rigid form insulation, shown inFigure3.5.

Figure 3.5: Storage tank

3.4 Pump

To circulate nanofluid from the storage tank to the absorber tube at some appreciable height, pump is used. In this experiment self priming moonset centrifugal pump is used. The pump used to carry out this experiment shown in the Figure3.6

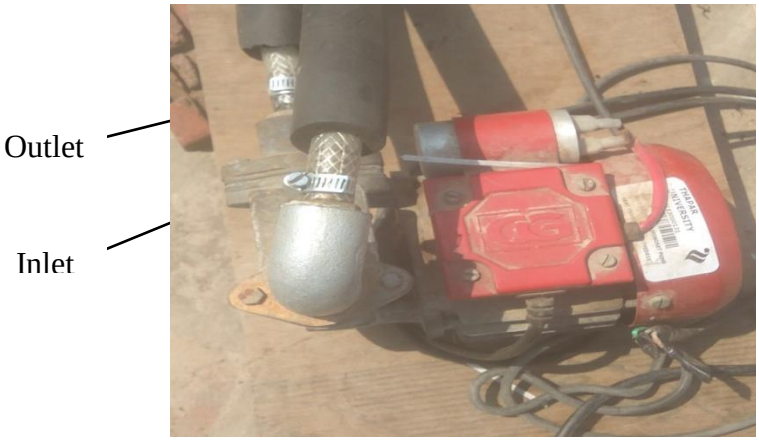

Figure 3.6 Pump

3.5 Specification of Experimental Setup

Table 3.1 Specification of PTC

S.No.	Components	
1	**Parabolic Reflector**	**Specification**
	Length	1.219 m
	Arc Length	1.829 m
	Depth	0.207 m
	Focal Length	0.607 m
	Material	SS with mirror film
	Tracker	Single axis (E-W)
	Reflectivity	0.84
2	**Absorber Tube**	**Specification**
	Length	1.219 m
	Inner Inlet Diameter	0.0381 m
	Inner Exit Diameter	0.019 m
	Absorber Tube material	Copper
	Insulation material	PUF

	Piping Material	GI and copper
3	**Storage Unit**	**Specification**
	Capacity	13 Liter
	Material	GI
	Insulation of Tank	Rigid foam
4	**Control Unit**	**Specification**
	Stepper Motor	1 (For Tracking)
	Power Rating	0.125 HP
	Head	12 m
5	**Sensing Element**	**Specification**
	RTD Sensor	To measure temperature
	Pyranometer	To measure solar radiation intensity

3.6 Measuring Instruments Used

3.6.1 Rotameter

Rotameters has been to measure the flow rate of fluid going to the absorber tube. The control valves are provided on the rotameter to regulate the flow of fluid into the system. Through this required flow rate of the fluid can be set for carrying out experiments. Its range is 100 to 1000LPH with least count of 25LPH.Figure 3.7 shows an image of rotameter used in the set up.

Figure 3.7:Rotameter

3.6.2 RTD Sensor

RTD sensors are used to measure temperature at different points in the Parabolic Trough Collector. The temperature sensors are placed at 2 different points, namely, the inlet and outlet of absorber tube. The readings from all the temperature sensors are displayed on a digital panel meter. The temperature at the required point can be noted by operating the selector switch present on the digital panel meter. Figure 3.8 shows the image of the digital panel meter used in the experiment

Figure 3.8: Digital panel meter.

3.6.3 Pyranometer

It is used to measure solar flux in w/m^2. The pyranometer used in experiments shown in Figure 3.9, is having sensitivity 7 to 14 μV/Wm^2, response time is less than 5 seconds, temperature dependence of sensitivity is less than 1 %, operational temperature range is -40^{o}C to +80^{o}C, maximum solar intensity is 4000 W/m^2, field of view is 180^o.

Figure 3.9: Payaranometer

3.7 Nanofluid Preparation

3.7.1 Weight of Nonoparticles

In this experiment, Al_2O_3 nanoparticle is dispersed in water, are prepared in three different concentrations (0.01%, 0.045% and.0.08%). The Amount of nanoparticles used for the preparation nanofluids was measured by the following expression:

$$W_{np} = V_{np} * \rho_{np} \quad (3.1)$$

$$V_{np} = \frac{V_{bf} * f_v}{100 - f_v} \quad (3.2)$$

Where W_{np} is Weight of nanoparticles, V_{np} is Volume of nanoparticles, ρ_{np}: Density of nanoparticles, V_{bf} Volume of base fluid, f_v is Concentration by volume

Density of Al_2O_3 nanoparticle = 3.92 gm/cm^3, Density of water = 1 gm/cm^3

Table 3.2: Mass Al_2O_3 nanoparticles in water as base fluids to make the nanofluids at three concentrations

VOLUME CONCENTRATION	MASS OF AL_2O_3 NANOFLUID
0.01%	3.17 gm
0.045%	14.29 gm
0.08%	25.42 gm

Required quantity of nanoparticles is weighed in the weighing machine shown in Figure 3.10

Figure 3.10: Weighing machine

After dispersion of nanoparticles, we need to treat the nanofluid in two equipments for the proper dispersion and stability of the nanoparticles in the base fluid. These equipments are

1. Magnetic Stirrer.
2. Sonicator

3.7.2 Magnetic Stirrer

For the proper dispersion of nanoparticles in the fluid magnetic stirrer is used. The magnetic stirrer bead is placed in the nanofluids. After that, the flask having nanofluids is placed on the disk of the magnetic stirrer and stirrer is turned on. The speed of mixing can be controlled by using a dimmer provided on the apparatus. The magnetic base of the stirrer and the magnetic stirrer bead have different poles. So, when the stirrer is turned on the magnetic stirrer, bead starts rotating and the nanoparticles start dispersing properly inside the flask. The Figure 3.11 below shows the magnetic stirrer and nanofluids present on it.

Figure 3.11: Magnetic stirrer.

After stirring, still there is a chance that nanoparticles will form agglomerate in the base fluid. So, to make sure that no agglomeration is formed, surfactants are used in nanofluids. Madhurseekole et al. (2010) suggested that for aluminum oxide oleic acid is best suited surfactant

Duangthongsuk and Wongwises (2009) also investigated that the surfactant does not effects the thermophysical properties of nanofluid when used at low concentration i.e. 0.01%. Hence, a low concentration of CTAB surfactant has been used during the stirring. A magnetic stirrer was operated for 30 minutes for every concentration.

3.7.3Sonicator

After magnetic stirring, there is still a chance of cluster formation or occurrence of sedimentation. So, to avoid this nanofluid are treated by using ultrasonic vibrator. Ultrasonic vibrators are of many types but we have used bath type sonicator here as shown in Figure 3.12

Figure 3.12: Sonicator

The ultrasonic vibration was continued for 90 minutes for each concentration at room temperature. Basically, the ultrasonic vibrate breaks the clusters formed in the nanofluids using sound energy. The speed of the vibration can be set according to the need.

3.8Experimentally measurement of thermo-physical properties of nanofluid

3.8.1 Density bottle

The density is measured using specific gravity bottle. It consists of a bottle in which the liquid of unknown density is poured. Then, the bottle is weighed with and without the liquid (shown in Figure3.13) and the difference between these two weights is then divided by the weight of an equal volume of water and the specific gravity of the liquid is obtained. The density bottle used in the experiments is of 25 ml capacity, so divide the difference in the weight of bottle by 25, as specific gravity of water is 1.

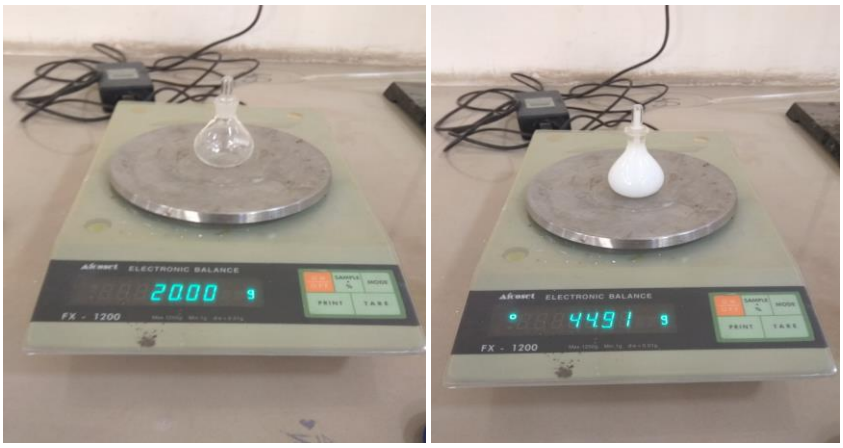

Figure 3.13: (a) Empty density bottle. (b) Filled density bottle

3.8.2 KD2 PRO meter

The thermal conductivity of the nanofluid is measured using KD2 Pro (Decan Devices, USA). The instrument has different sensors meant for different purposes. Here, KS-1 sensor needle (shown in Figure 3.14) was used for measuring the thermal conductivity. The sensor needle is made up of stainless steel having diameter of 1.3mm and length of 60mm. SH-1 sensor needle was used for measuring volumetric specific heat. For having the accurate results the needle should be in same place i.e. it shouldn't be disturbed. The instrument was calibrated using the glycerin liquid available with the instrument set only and values were matched with the manual present inside the instrument set. The correctness in measurement was in the acceptable range of 0.3-3 w/mk which matches with that of ASTM56 and 1EEE57 standards. The thermal conductivity of water has also been measured and was checked against the standard data.

While performing the experiments, the needle was kept vertically in a tube using a holder. The gap between the two readings of the thermal conductivity should be at least 15 minutes. As the needle works by heating the liquid, so there is some time needed for cooling down. There is also an automatic mode present in the instrument which automatically measures the values and keep recording after a minimum time interval. Also, there comes an error value with every thermal conductivity value. The error value should be less than permissible value i.e. 0.0100 for every reading.

Figure 3.14: KS-1 sensor

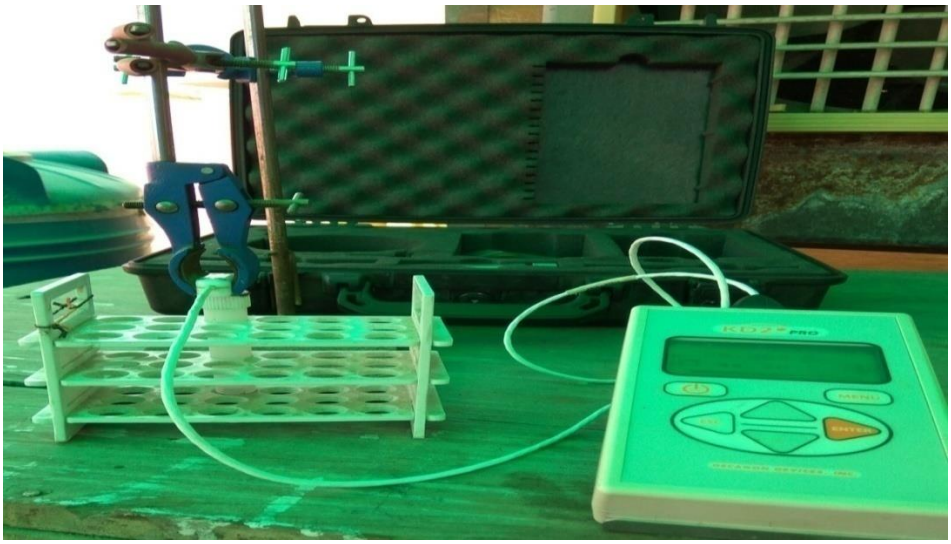

Figure 3.15: Kd2 pro thermal property analyzer setup with Al_2O_3-H_2O nanofluid.

3.8.4 Viscosity measurement

The viscosity measurement was done using Anton Paar Rheometer shown in Figure 3.16. The instrument was connected to computer where all the values of viscosity were stored. The viscosity of the samples was measured at different concentrations. The device needs to be connected to the bath tub for getting changes in temperature of the fluid. The device needs to be cleaned after every sample reading.

Figure 3.16: Reo-meter

3.8.3 Ph meter

Ph meter is use to measure the ph value of any fluid. A digital ph meter is used to measure ph value of nanofluids is shown in Figure 3.17, is having range of 0 to 14, accuracy of ± 0.02 ph with least count of 0.01.

Figure 3.17: Ph meter

3.9 Experimental Procedure

Following are the steps followed to conduct the experiments

Step 1 Preparation of nanofluids of required volumetric concentration.

Step 2 Take a sample of nanofluids to check density, thermal conductivity and ph.

Step 3 Cleaning of tank and pouring of nanofluid in the tank.

Step 4 Rotate the reflector sheet with the help of tracker and set it on -35^0(east) with the help of compass.

Step 5 Start pump and set required mass flow rate with the help of one way ball valve and rotameter.

Step 6 Check the flow rate manually with stop watch and five liter container, if flow rate is correct then go for next step, otherwise with the help of flow control valve change the flow rate and again check flow rate manually.

Step 7 Switch on the tracker at 10.00AM.

Step 8 Note down temperature reading at the inlet and outlet of absorber tube after every half an hour.

Step 9 Take sample of nanofluid at 10.00AM, 11.00AM, 12.00AM, 1.00PM, 2.30PM to check the density and ph of nanofluids.

Step 10 Take samples of nanofluid at 10.30AM, 11.30AM, 12.30PM, 1.30PM, 2.30PM to check its thermal conductivity.

Chapter 4

Results and Discussion

4.1 Governing Equations for Efficiency Calculation

To check the performance of solar heat collector a few parameters are to be calcukated like useful heat gain, instantaneous efficiency, thermal efficiency. Following are the equations used to calculate these parameters

1) **Useful heat gain**

$$q_u = \dot{m} C_p (T_{out} - T_{in}) \quad (4.5)$$

2) **Instantaneous Efficiency**

$$\eta_i = \frac{\dot{m} C_p (T_{out} - T_{in})}{G_t W L} \quad (4.6)$$

3) **Thermal Efficiency**

$$\eta_t = \frac{\dot{m} C_p (T_{out} - T_{in})}{G_t A_{aper}} \quad (4.7)$$

Where η_i is instantaneous efficiency, η_t is thermal efficiency, $\dot{m}$ mass flow rate in kg/s, C_p is specific heat J/kg k, T_{in} is temperature at the inlet of absorber tube, T_{out} is temperature at the outlet of absorber tube, G_t is global solar intensity in W/m^2, A_{aper} is aperture area of collector in m^2, W is width collector in m, L length of collector in m.

4.2 Thermophysical Properties of Nanofluid

Thermophysical of working fluid are very important while investigating the performance of nanofluid based solar heat collector. These properties effect the performance of solar collector. Thermophysical properties of nanofluid vary with time and temperature. Some of the models proposed by researchers are discussed.

4.2.1 Thermal conductivity [26]

$$K_{eff} = \left(\frac{K_{np}+2K_{bf}+2f_v(K_{np}+K_{bf})}{K_{np}+2K_{bf}-f_v(K_{np}-K_{bf})}\right) * K_{bf} \quad (4.2)$$

Where K_{nf}, K_{np}, K_{bf} are the thermal conductivity of nanofluid, nanoparticle, basefluid respectively.

4.2.2 Viscosity [27]

$$\mu_{nf} = \frac{\mu_{bf}}{(1-f_v)^{2.5}} \quad (4.4)$$

Where μ_{nf}, μ_{bf} are dynamic viscosity of nanofluid, basefluid respectively.

4.2.3 Specific heat [27]

$$C_{p,np} = C_{p,np}f_v + C_{p,bf}(1-f_v) \quad (4.3)$$

Where f_v is volumetric concentration of nanofluid, $C_{p,nf}$, $C_{p,np}$, $C_{p,bf}$, is specific heat of nanofluid, nanoparticle, basefluid respectively.

4.2.4 Density [27]

$$\rho_{nf} = f_v\rho_{np} + (1-f_v)\rho_{bf} \quad (4.1)$$

Where ρ_{nf}, ρ_{np}, ρ_{bf} are the density of nanofluid, density of nanoparticle, density of base fluid in g/cm^3 respectively.

4.3 Solar Intensity Received

Variation in the Solar Intensity in the month of April, May, June with time of the day is shown in the Figure4.1 to 4.3

1) Variation in Solar Intensity in the month of April

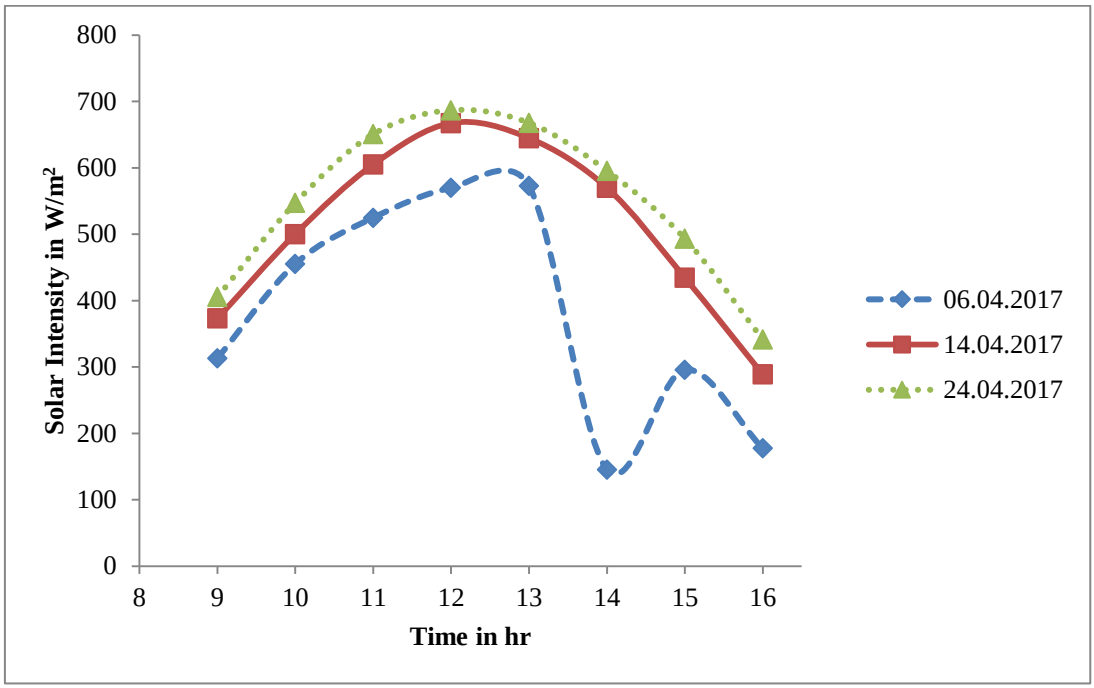

Figure4.1: Variation in Solar Intensity on 6th, 14th, 24th of April.

2) Variation in solar Intensity in the month of May.

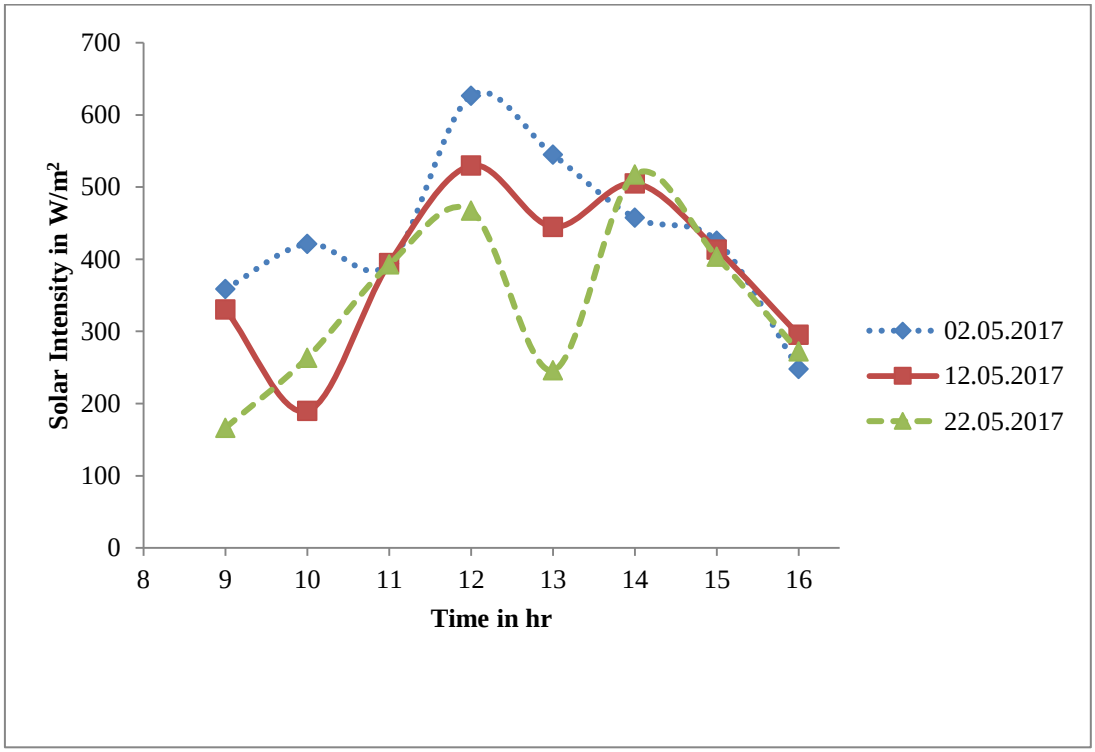

Figure4.2: Variation in Solar Intensity on 2nd,12th, 22nd of May.

3) Variation in solar Intensity in the month of June.

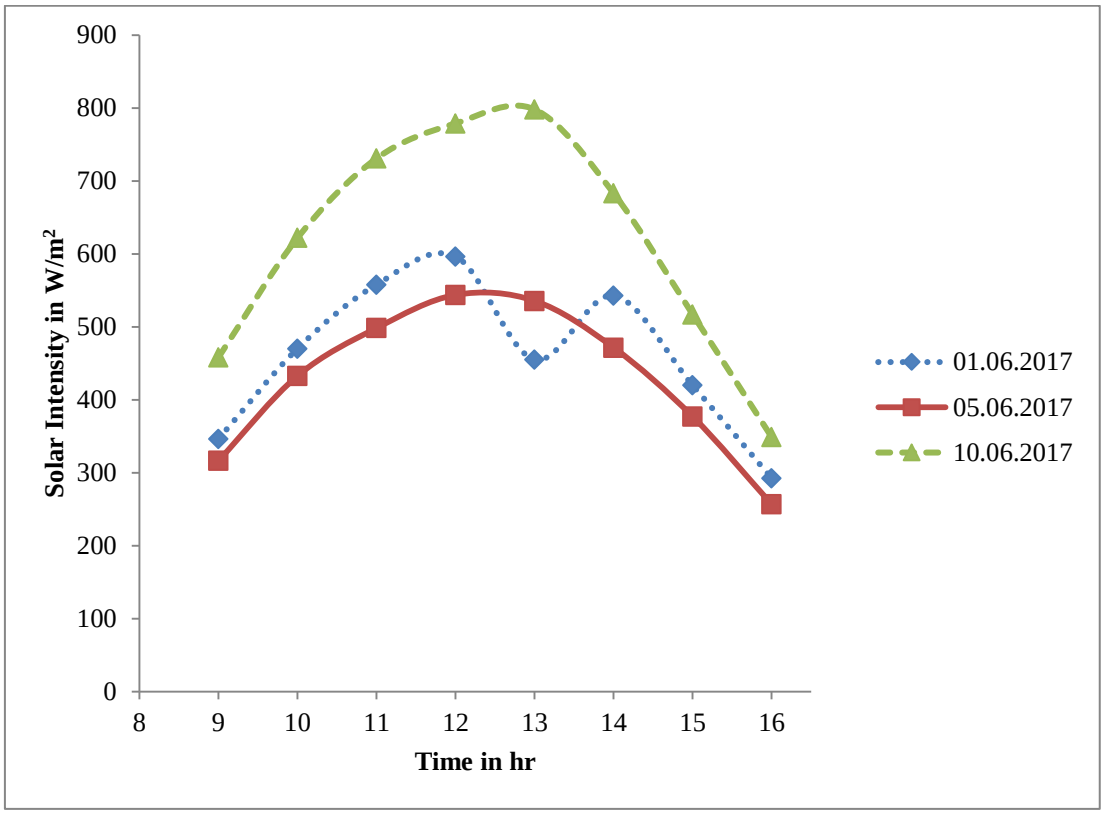

Figure4.3: Variation in Solar Intensity on 1st, 5th, 10th of June.

In the above graphs it is seen that in the month of April solar intensity varies from 200 W/m^2 to 650 W/m^2. In the month of May it varies from 150W/m^2 to 600W/m^2 and in the month of June it varies from 300W/m^{2}to 750 W/m^2. It is observed that that a good solar intensity is received between 10.00 am to 3.00 pm. It is also observed that there are sudden drops in the curves that are due to cloudy weather.

4.4Variation of Instantaneous Efficiency for various working fluids during day time (10.00 hr to 14.30 hr)

The variation in instantaneous efficiency for Al_2O_3-H_2O nanofluids of different volumetric concentrations (0.01%, 0.045%) at different mass flow rate (150LPH, 200LPH), in convergent absorber tube and straight absorber tube has been shown in Figure 4.4, 4.5, 4.6 &4.7.

1) Variation of Instantaneous Efficiency at 150 LPH with Al_2O_3-H_2O nanofluids of volumetric concentration 0.01% in straight absorber tube and convergent absorber tube.

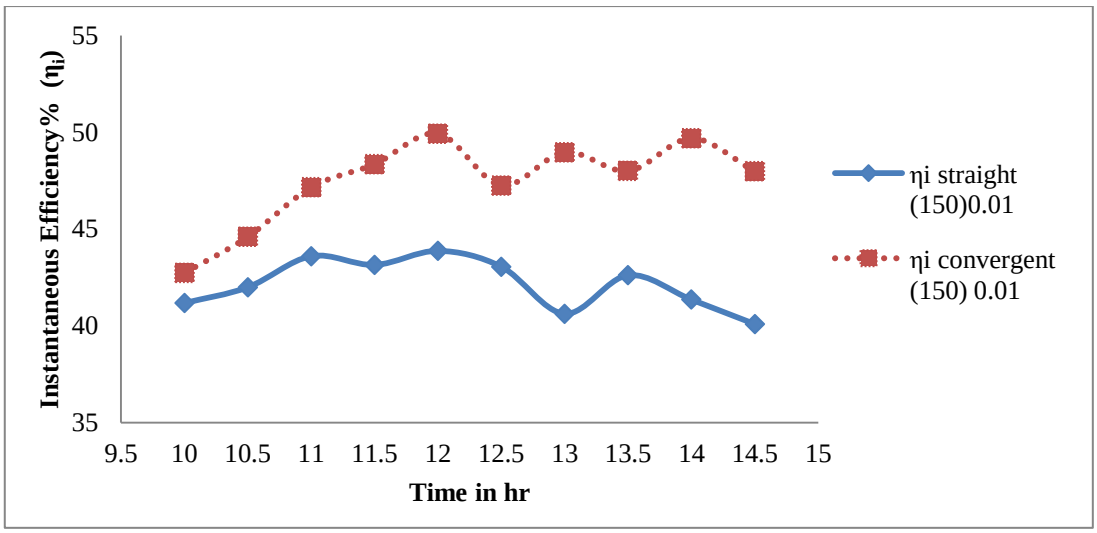

Figure4.4: Variation of Instantaneous Efficiency at 150 LPH with Al_2O_3-H_2O(0.01%) nanofluids in straight absorber tube and convergent absorber tube.

2) Variation of Instantaneous Efficiency at 200 LPH with Al_2O_3-H_2O nanofluids of volumetric concentration 0.01% in straight absorber tube and convergent absorber tube.

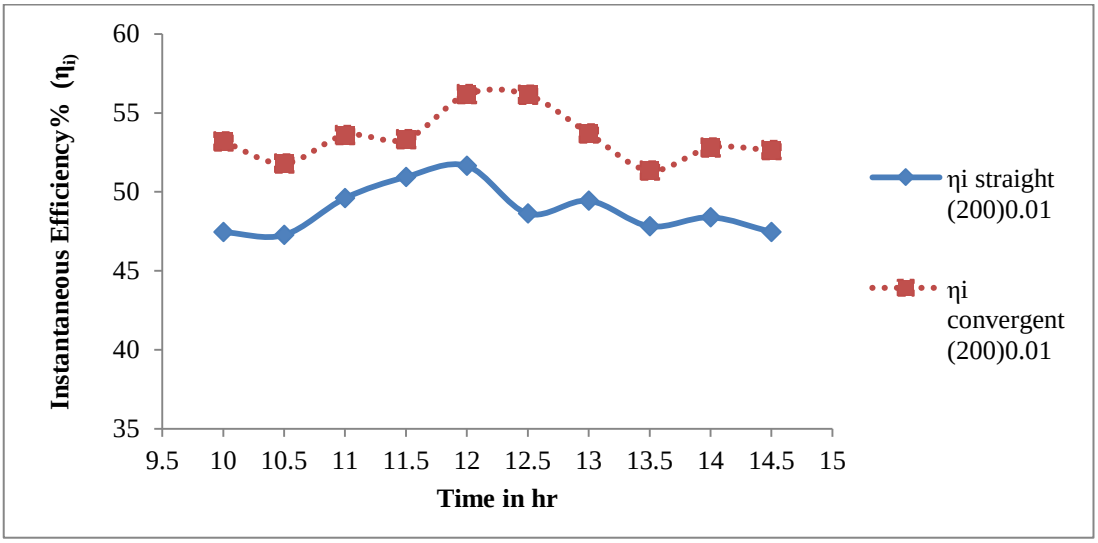

Figure4.5:Variation of Instantaneous Efficiency at 200 LPH with Al_2O_3-H_2O(0.01%) nanofluids in straight absorber tube and convergent absorber tube.

3) Variation of Instantaneous Efficiency at 150 LPH with Al_2O_3-H_2O nanofluids of volumetric concentration 0.045% in straight absorber tube and convergent absorber tube.

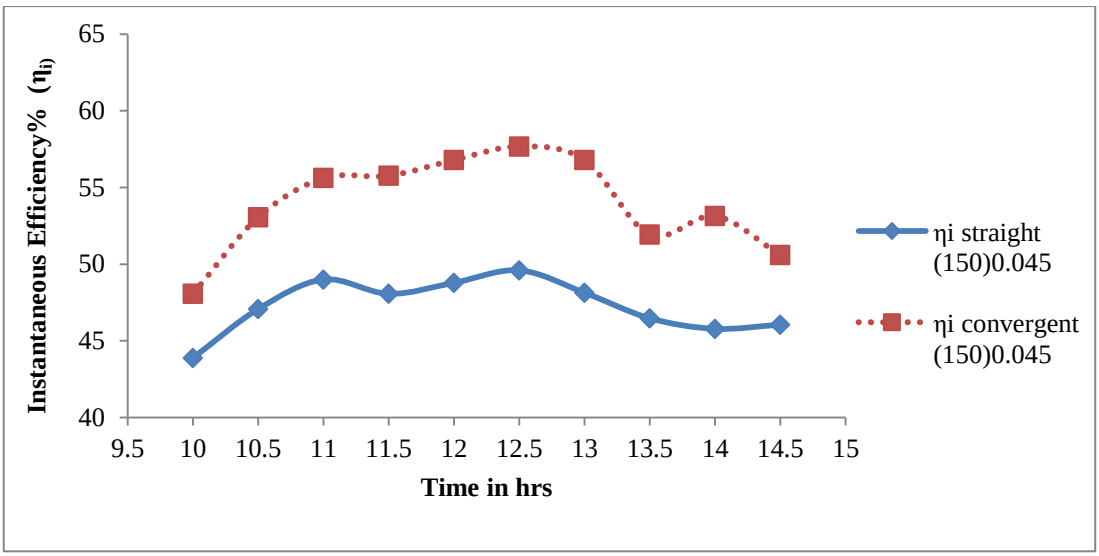

Figure4.6: Variation of Instantaneous Efficiency at 150 LPH with Al_2O_3-H_2O (0.045%) nanofluids in straight absorber tube and convergent absorber tube.

4) Variation of Instantaneous Efficiency at 200 LPH with Al_2O_3-H_2O nanofluids of volumetric concentration 0.045% in straight absorber tube and convergent absorber tube.

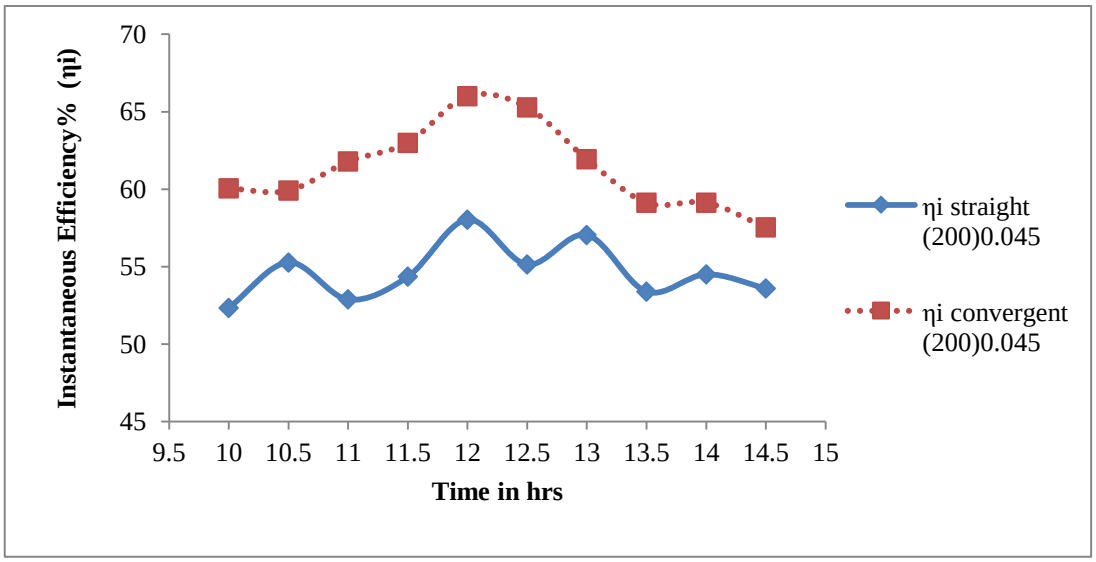

Figure4.7: Variation of Instantaneous Efficiency at 200 LPH with Al_2O_3-H_2O(0.045%) nanofluids in straight absorber tube and convergent absorber tube.

It has been observed from above Figure no. 4.4, 4.5, 4.6 & 4.7 in above Figures that in convergent absorber tube instantaneous efficiency isslightly more (5% to 10%) than that of straight absorber tube, for Al_2O_3–H_2O nanofluids of 0.01% and 0.045% volumetric concentration at 150LPH and 200LPH mass flow rate.In straight absorber tube around 58% and 51% is maximum instantaneous efficiency is observed with 0.045% volumetric concentration, at 150LPH and 200LPH, respectively.

Graphs of variation of instantaneous efficiency for various working fluids like water and Al_2O_3 – H_2O nanofluids of different volumetric concentrations (0.01%, 0.045%, 0.08%) at different mass flow rate (150LPH, 200LPH, 250LPH), in convergent absorber tube was observer in Figure4.8 to 4.13.

5) Variation of Instantaneous Efficiency at 150 LPH with water and Al_2O_3-H_2O nanofluids with different volumetric concentration (0.01%, 0.045%, 0.08%) in convergent absorber tube.

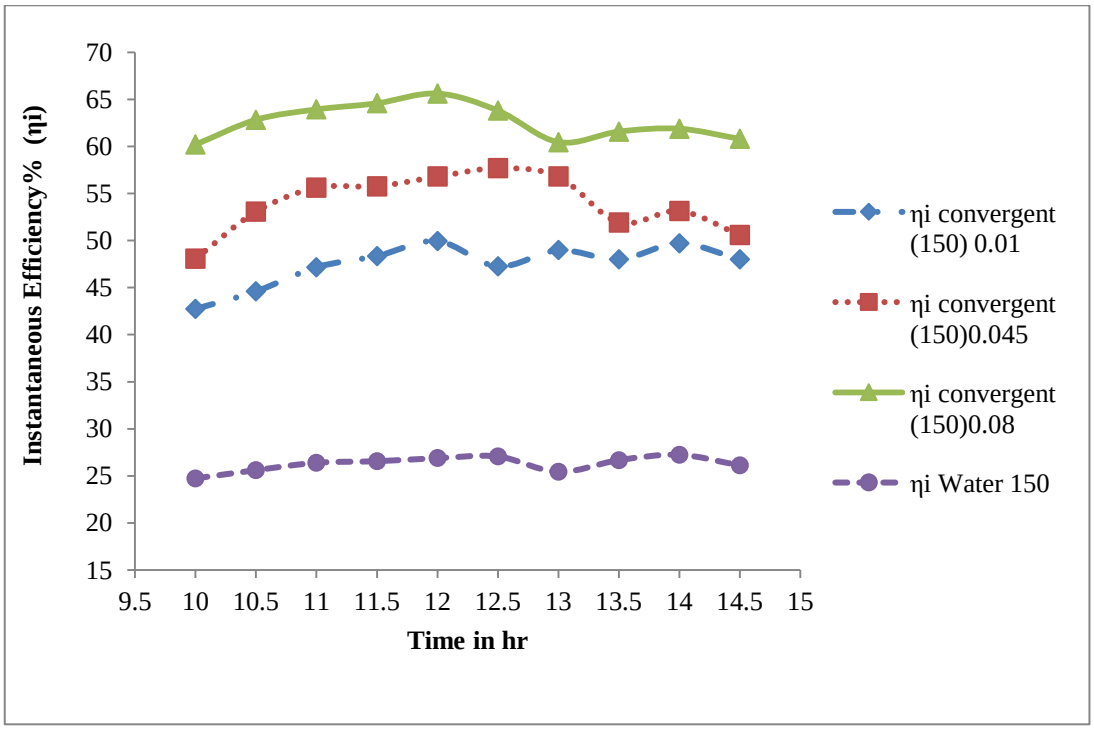

Figure4.8: Variation of Instantaneous Efficiency at 150 LPH with water and Al_2O_3-H_2O nanofluids with different volumetric concentration.

6) Variation of Instantaneous Efficiency at 200 LPH with water and Al_2O_3-H_2O nanofluids with different volumetric concentration (0.01%, 0.045%, 0.08%) in convergent absorber tube.

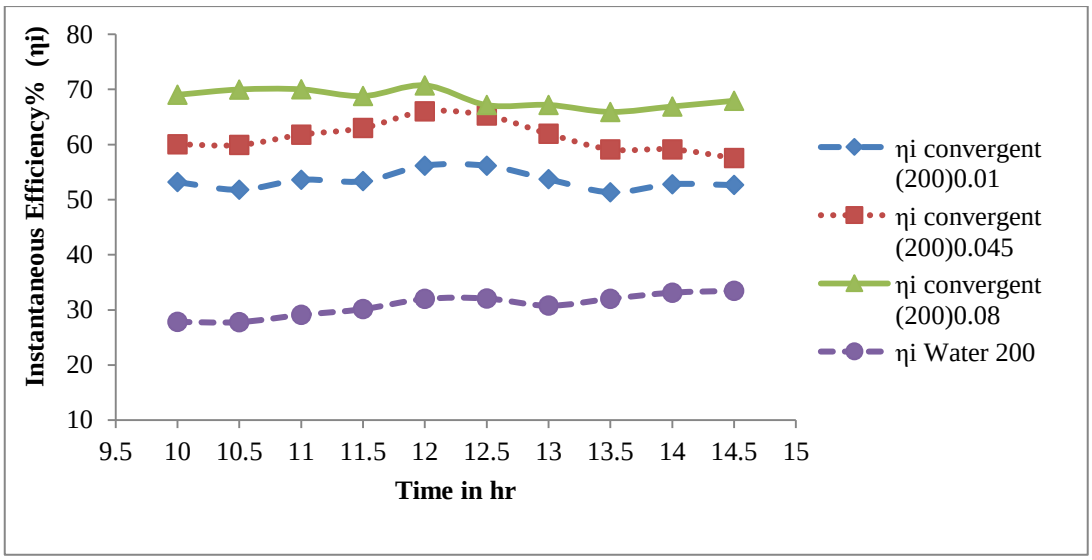

Figure4.9: Variation of Instantaneous Efficiency at 200 LPH with water and Al_2O_3-H_2O nanofluids with different volumetric concentration.

7) Variation of Instantaneous Efficiency at 250 LPH with water and Al_2O_3-H_2O nanofluids with different volumetric concentration (0.01%, 0.045%, 0.08%) in convergent absorber tube.

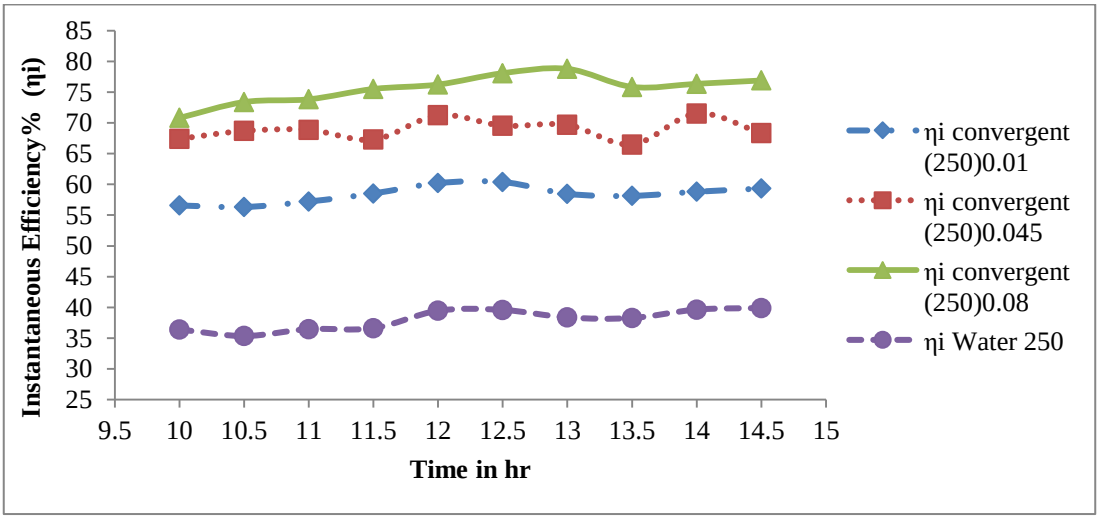

Figure4.10: Variation of Instantaneous Efficiency at 250 LPH with water and Al_2O_3-H_2O nanofluids with different volumetric concentration.

It is observed from the Figures that instantaneous efficiency increases with increase in volumetric concentration. With mass flow rate of 150 LPH, maximum instantaneous efficiencies are around 49%, 57% and 65% with concentration ofAl_2O_3-H_2O 0.01%, 0.045% and 0.08% respectively. This is due to the fact that with increase in volumetric concentration of nanoparticles thermal conductivity of nanofluids increases. Maximum instantaneous efficiency for water is around 39%, at mass flow rate of 250LPH.

8) Variation of Instantaneous Efficiency of Al_2O_3-H_2O nanofluids with volumetric concentration 0.01% at different flow rate (150LPH, 200LPH, 250LPH) in convergent absorber tube.

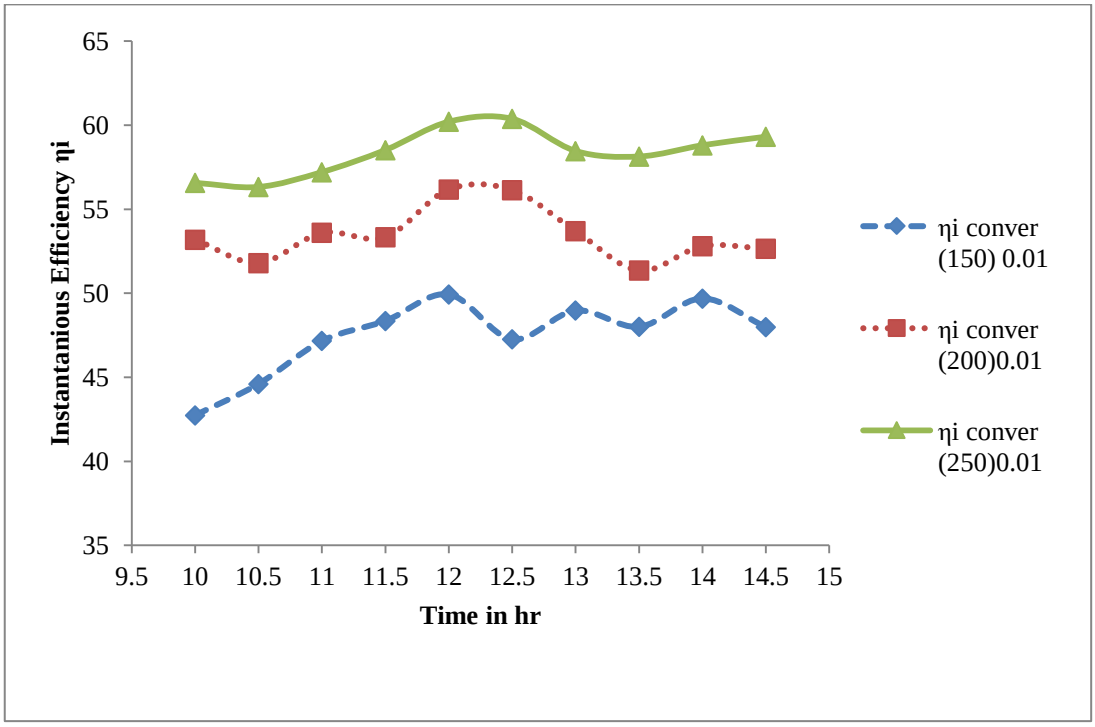

Figure4.11: Variation of Instantaneous Efficiency of Al_2O_3-H_2O nanofluidswith volumetric concentration of 0.01% at different mass flow rates.

9) Variation of Instantaneous Efficiency of Al_2O_3-H_2O nanofluids with volumetric concentration 0.045% at different flow rate (150LPH, 200LPH, 250LPH) in convergent absorber tube.

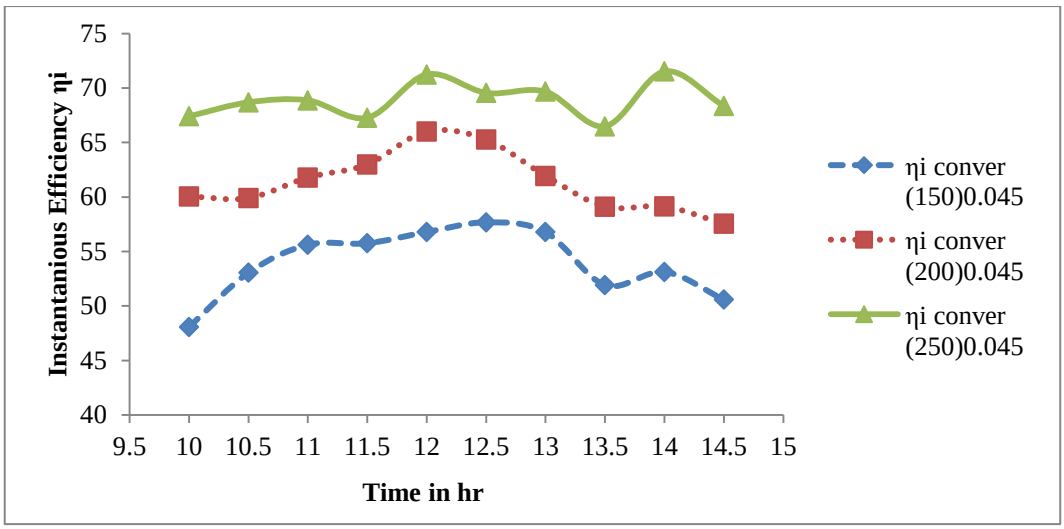

Figure4.12: Variation of Instantaneous Efficiency of Al_2O_3-H_2O nanofluids with volumetric concentration of 0.045% at different mass flow rates.

10) Variation of Instantaneous Efficiency of Al_2O_3-H_2O nanofluids with volumetric concentration 0.08% at different flow rate (150LPH, 200LPH, 250LPH) in convergent absorber tube.

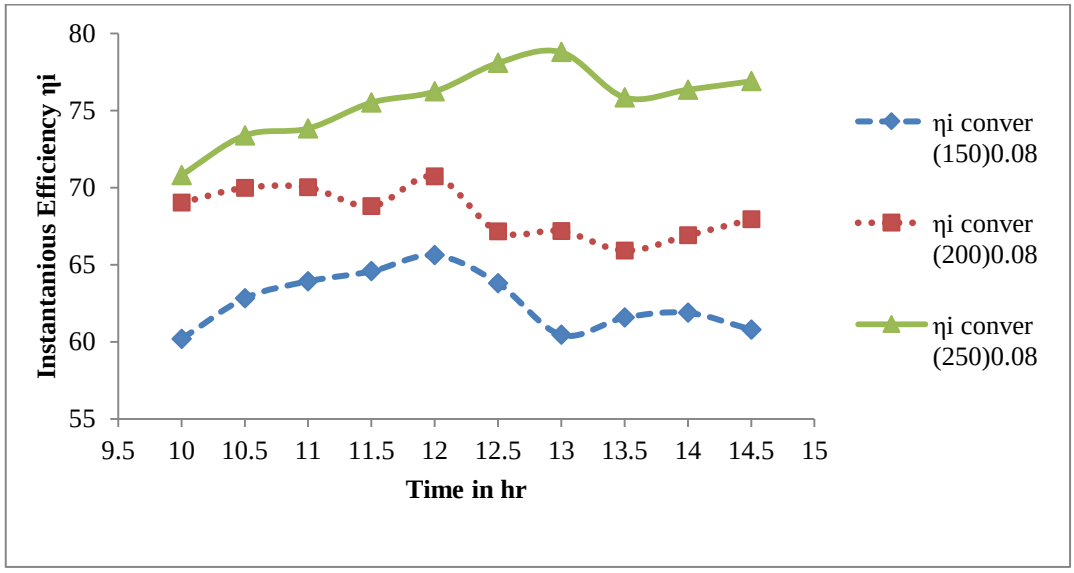

Figure4.13: Variation of Instantaneous Efficiency of Al_2O_3-H_2O nanofluids with volumetric concentration of 0.08% at different mass flow rates.

It is seen in the above Figures 4.11 to 4.13 that with increase in mass flow rate instantaneous efficiency increases. At the concentration of 0.08%Al_2O_3-H_2O, maximum instantaneous efficiencies are around 65%, 70% and 78%, with mass flow rate of 150 LPH, 200 LPH and 250 LPH respectively. This is because with increase in mass flow rate radiation losses decreases.

4.5Variation of Thermal Efficiency for various working fluid during day time (10.00 hr to 14.30 hr)

Variation of thermal efficiency for Al_2O_3 – H_2O nanofluids of different volumetric concentrations (0.01%, 0.045%) at different mass flow rate (150LPH, 200LPH), in convergent absorber tube and straight absorber tube was observer in Figure4.14, 4.15, 4.16 and4.17.

1) Variation of Thermal Efficiency at 150 LPH with Al_2O_3-H_2O nanofluids of volumetric concentration 0.01% in straight absorber tube and convergent absorber tube.

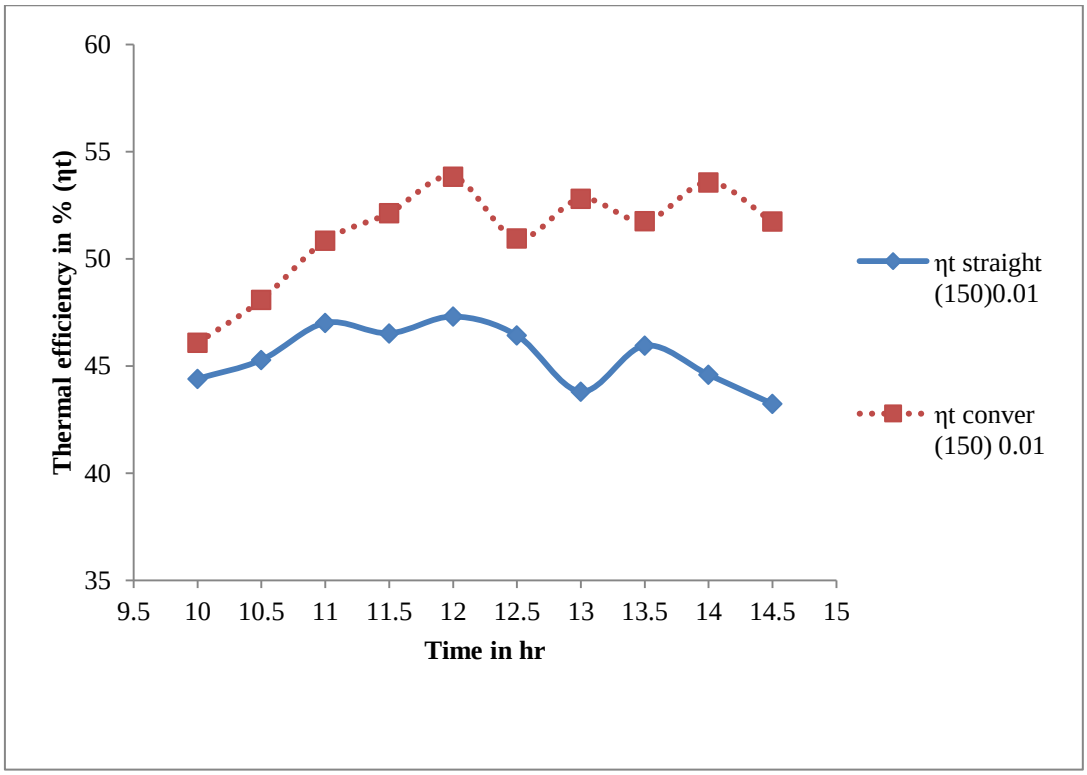

Figure4.14: Variation of Thermal Efficiency at 150 LPH with Al_2O_3-H_2O (0.01%) nanofluids in straight absorber tube and convergent absorber tube.

2) Variation of Thermal Efficiency at 200 LPH with Al_2O_3-H_2O nanofluids of volumetric concentration 0.01% in straight absorber tube and convergent absorber tube.

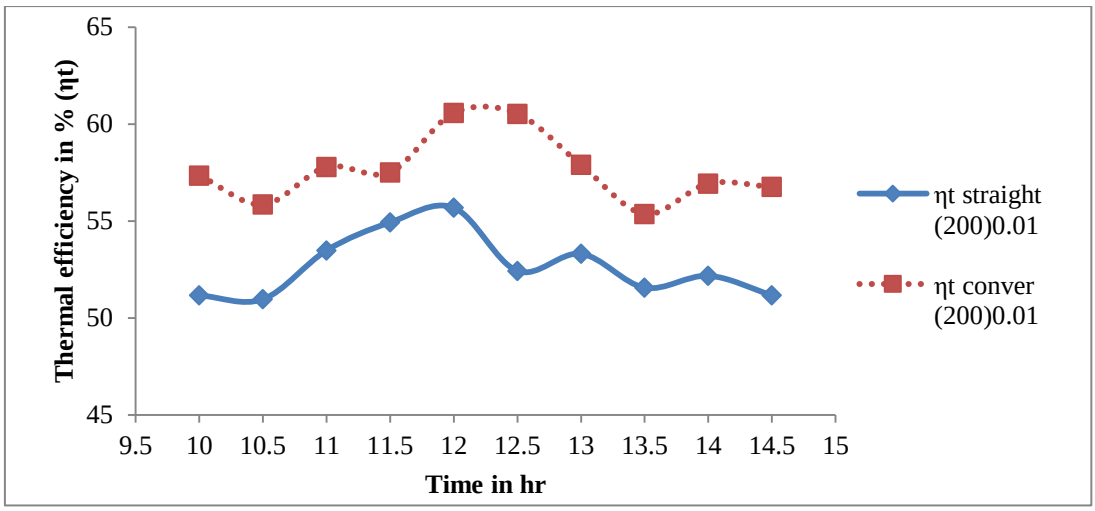

Figure4.15:Variation of Thermal Efficiency at 200 LPH with Al_2O_3-H_2O(0.01%) nanofluids in straight absorber tube and convergent absorber tube.

3) Variation of Thermal Efficiency at 150 LPH with Al_2O_3-H_2O nanofluids of volumetric concentration 0.045% in straight absorber tube and convergent absorber tube.

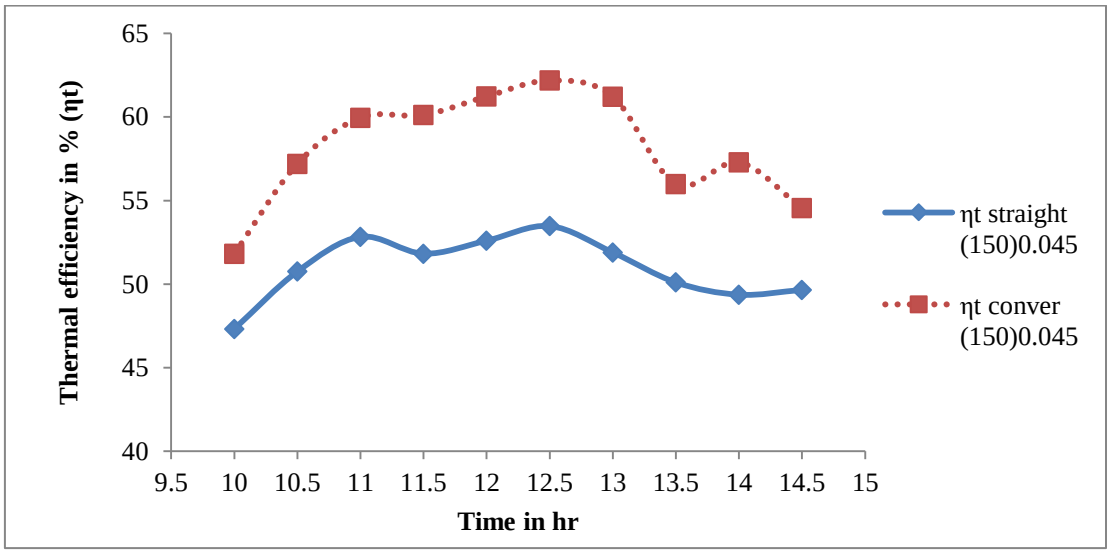

Figure4.16: Variation of Thermal Efficiency at 150 LPH with Al_2O_3-H_2O(0.045%) nanofluids in straight absorber tube and convergent absorber tube.

4) Variation of Thermal Efficiency at 200 LPH with Al_2O_3-H_2O nanofluids of volumetric concentration 0.045% in straight absorber tube and convergent absorber tube.

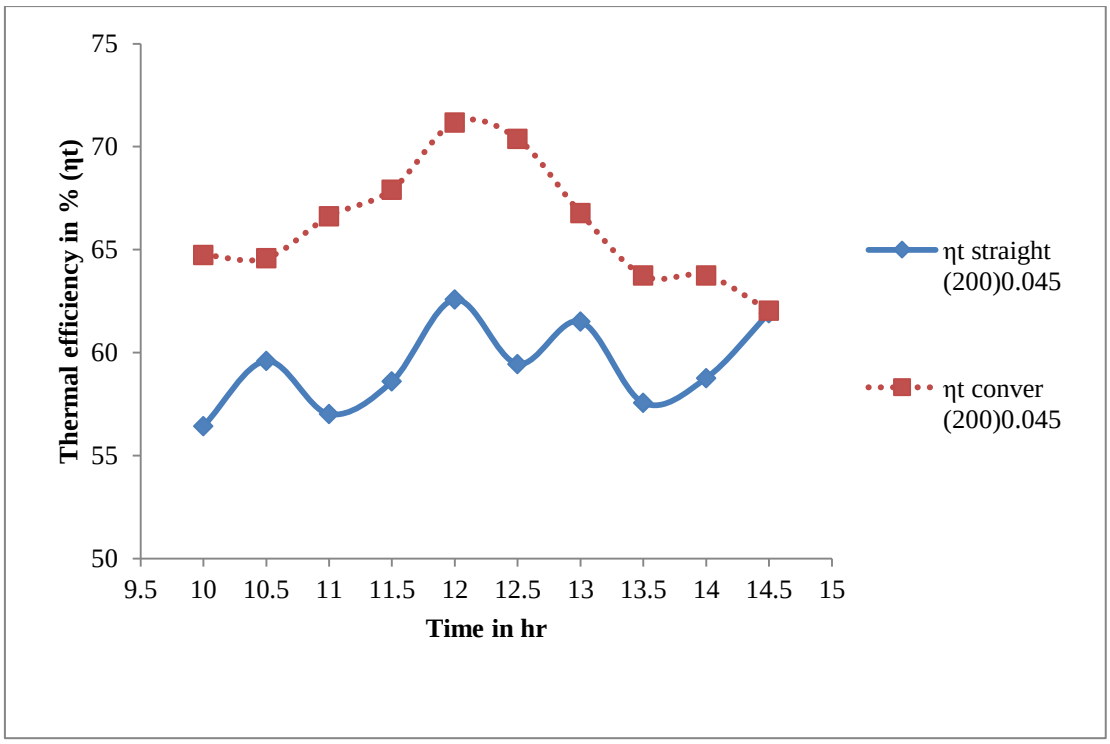

Figure4.17: Variation of Thermal Efficiency at 200 LPH with Al_2O_3-H_2O(0.045%) nanofluids in straight absorber tube and convergent absorber tube.

It is observed that maximum thermal efficiency is attained between 11.30 am to 12.30 pm. Thermal efficiency for convergent absorber tube is around 10% more than that of straight absorber tube with volumetric concentration of 0.045%Al_2O_3-H_2O, at mass flow rate of 200LPH. Maximum thermal efficiency for the straight tube is 62% with 0.045% Al_2O_3-H_2Ovolumetric concentration, at mass flow rate of 200 LPH.

Variation of thermal efficiency for various working fluids like water and Al_2O_3 – H_2O nanofluids of different volumetric concentrations (0.01%, 0.045%, 0.08%) at different mass flow rate (150LPH, 200LPH, 250LPH), in convergent absorber tube absorber tube is observer in Figure4.18 to 4.23.

5) Variation of Thermal Efficiency at 150 LPH with water and Al_2O_3-H_2O nanofluids with different volumetric concentration (0.01%, 0.045%, 0.08%) in convergent absorber tube.

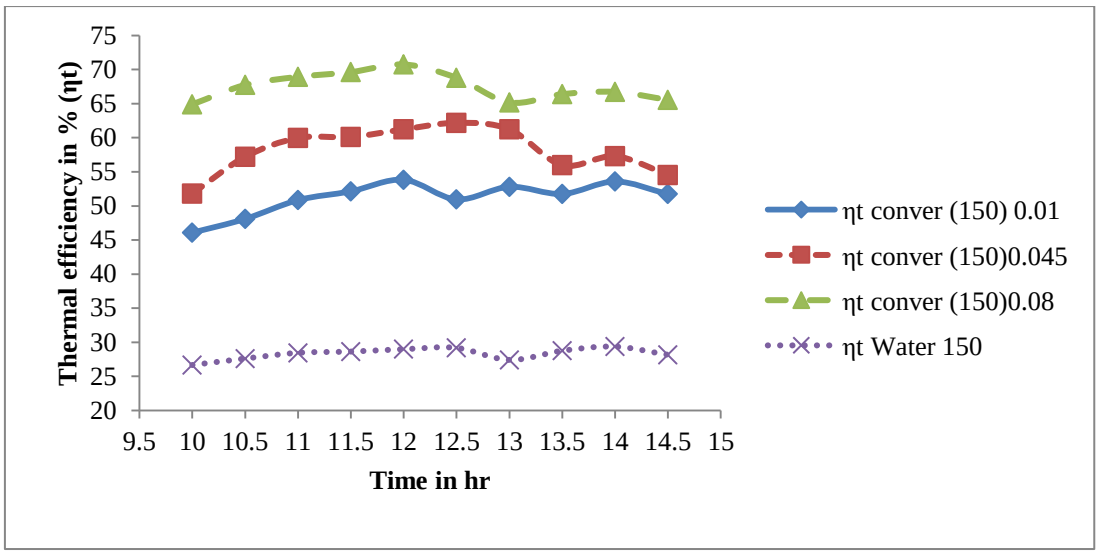

Figure4.18: Variation of Thermal Efficiency at 140 LPH with water and Al_2O_3-H_2O nanofluids with different volumetric concentration.

6) Variation of Thermal Efficiency at 200 LPH with water and Al_2O_3-H_2O nanofluids with different volumetric concentration (0.01%, 0.045%, 0.08%) in convergent absorber tube.

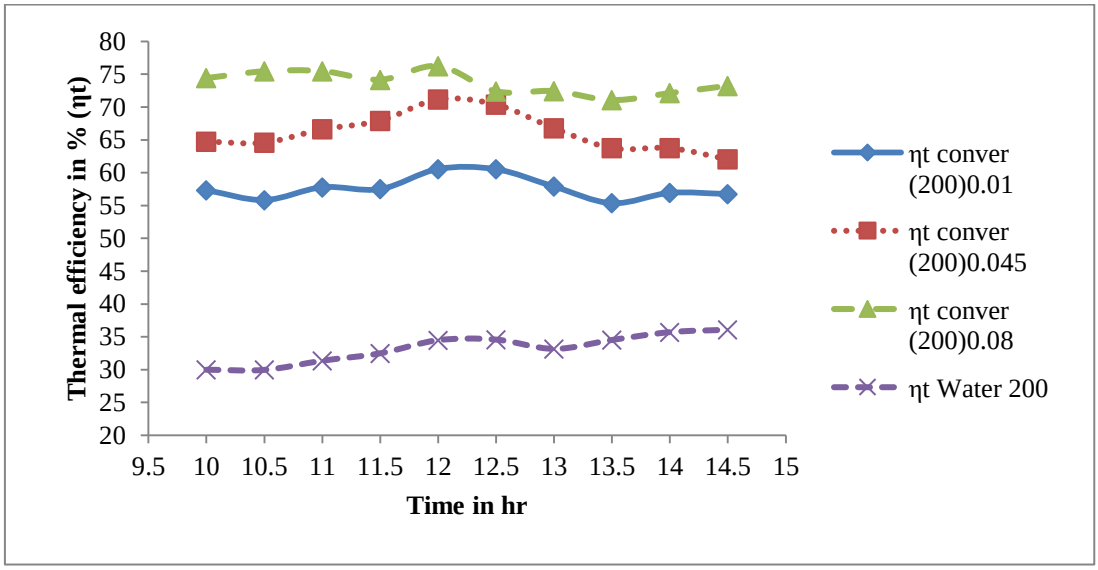

Figure4.19: Variation of ThermalEfficiency at 200 LPH with water and Al_2O_3-H_2O nanofluids with different volumetric concentration.

7) Variation of Thermal Efficiency at 250 LPH with water and Al_2O_3-H_2O nanofluids with different volumetric concentration (0.01%, 0.045%, 0.08%) in convergent absorber tube.

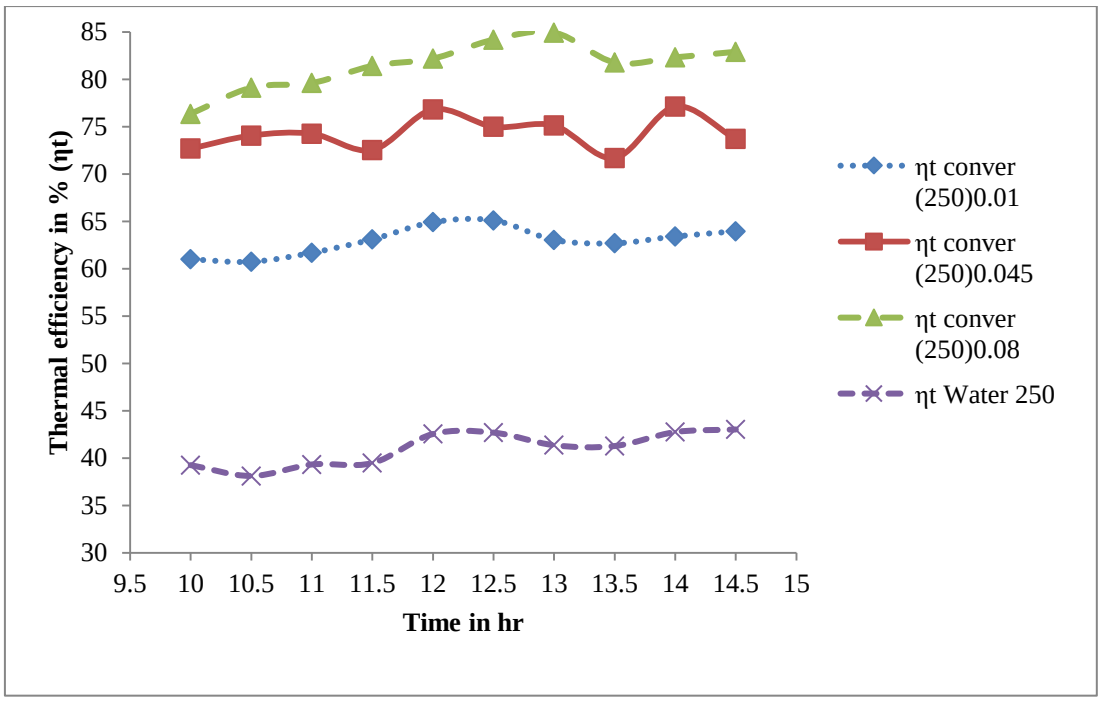

Figure4.20: Variation of Thermal Efficiency at 250 LPH with water and Al_2O_3-H_2O nanofluids with different volumetric concentration.

It is observed that maximum thermal efficiency is around 70%, 76% and 84% with 0.08% Al_2O_3-H_2O concentration at 150 LPH, 200LPH and 250LPH respectively. Whereas for water, it is seen that maximum thermal efficiency is around 29%, 36% and 43% at 150 LPH, 200LPH and 250LPH respectively.

8) Variation of Thermal Efficiency of Al_2O_3-H_2O nanofluids with volumetric concentration 0.01% at different flow rate (150LPH, 200LPH, 250LPH) in convergent absorber tube.

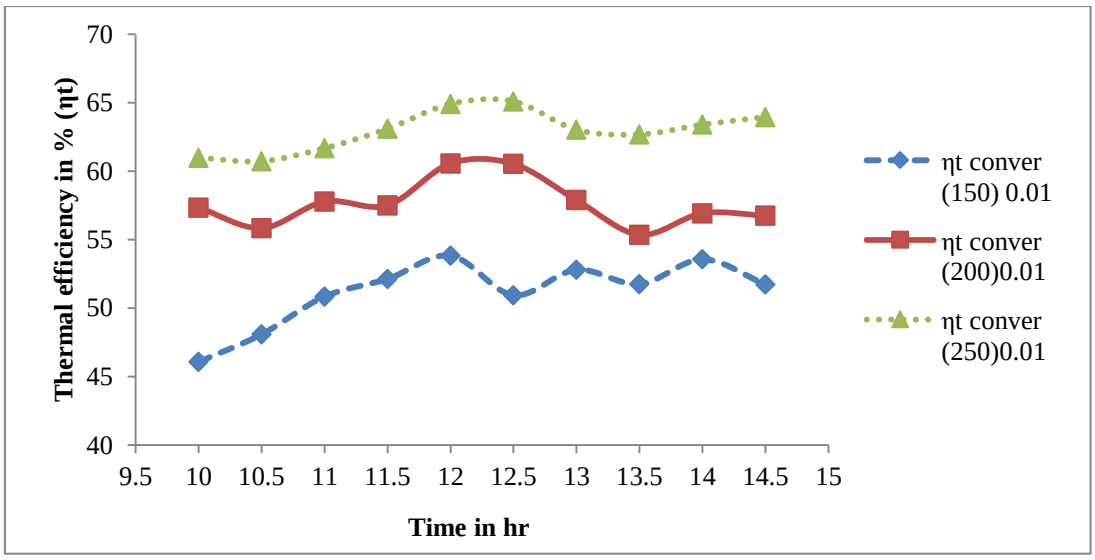

Figure4.21: Variation of Thermal Efficiency of Al_2O_3-H_2O nanofluids with volumetric concentration of 0.01% at different mass flow rates.

9) Variation of Thermal Efficiency of Al_2O_3-H_2O nanofluids with volumetric concentration 0.045% at different flow rate (150LPH, 200LPH, 250LPH) in convergent absorber tube.

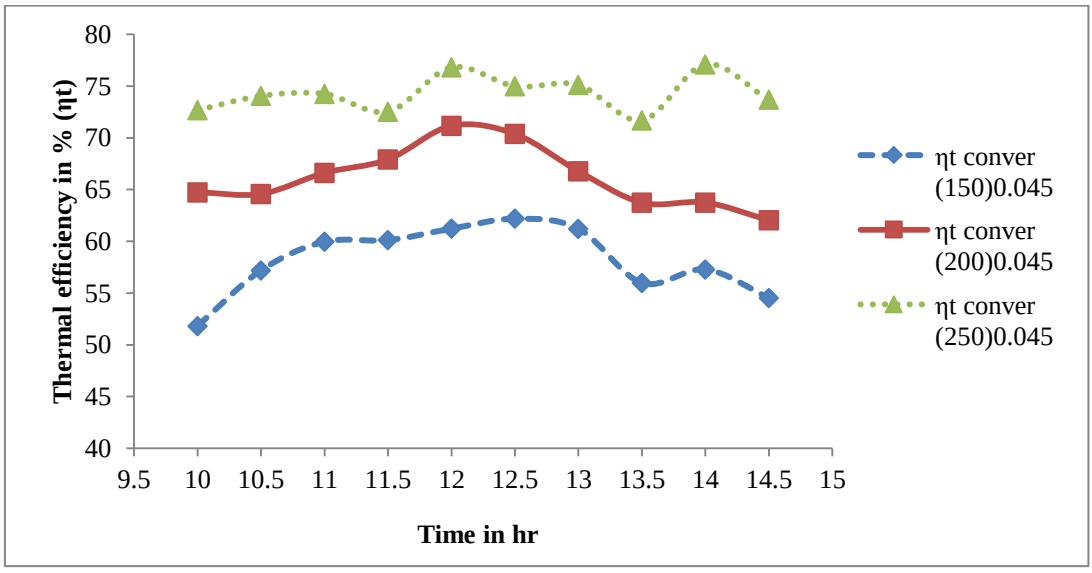

Figure4.22: Variation of Thermal Efficiency of Al_2O_3-H_2O nanofluids with volumetric concentration of 0.045% at different mass flow rates.

10) Variation of Thermal Efficiency of Al_2O_3-H_2O nanofluids with volumetric concentration 0.08% at different flow rate (150LPH, 200LPH, 250LPH) in convergent absorber tube.

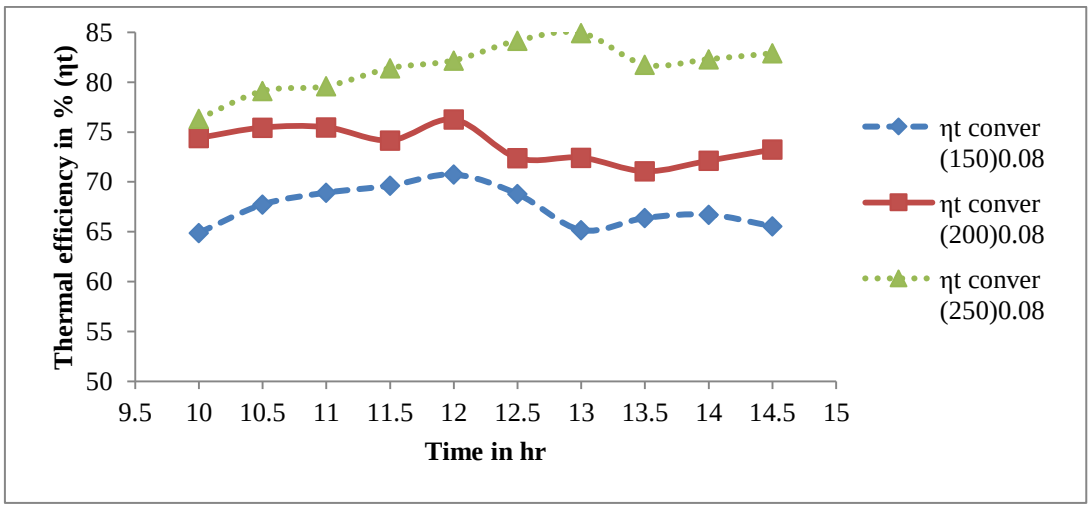

Figure4.23: Variation of Thermal Efficiency of Al_2O_3-H_2O nanofluids with volumetric concentration of 0.08% at different mass flow rates.

It is seen in the above Figures 4.2 to 4.23 that with increase in mass flow rate thermal efficiency increases. At the concentration of 0.045%Al_2O_3-H_2O, maximum thermal efficiencies are around 62%, 71% and 77%, with mass flow rate of 150 LPH, 200 LPH and 250 LPH respectively.

4.6 Variation in Thermophysical Properties of Al_2O_3-H_2O nanofluids.

4.6.1 Variation in Density

Graphs of variation in DensityAl_2O_3-H_2O nanofluids are observed with time of the day, at different mass flow rate (150LPH, 200LPH, 250LPH) and at different volumetric concentration (0.01%, 0.045%, 0.08%) are shown in Figure 4.24 to 4.26.

1) Variation in Density of Al_2O_3-H_2O nanofluids of different volumetric concentration (0.01%, 0.045%, 0.08%) at 150LPH.

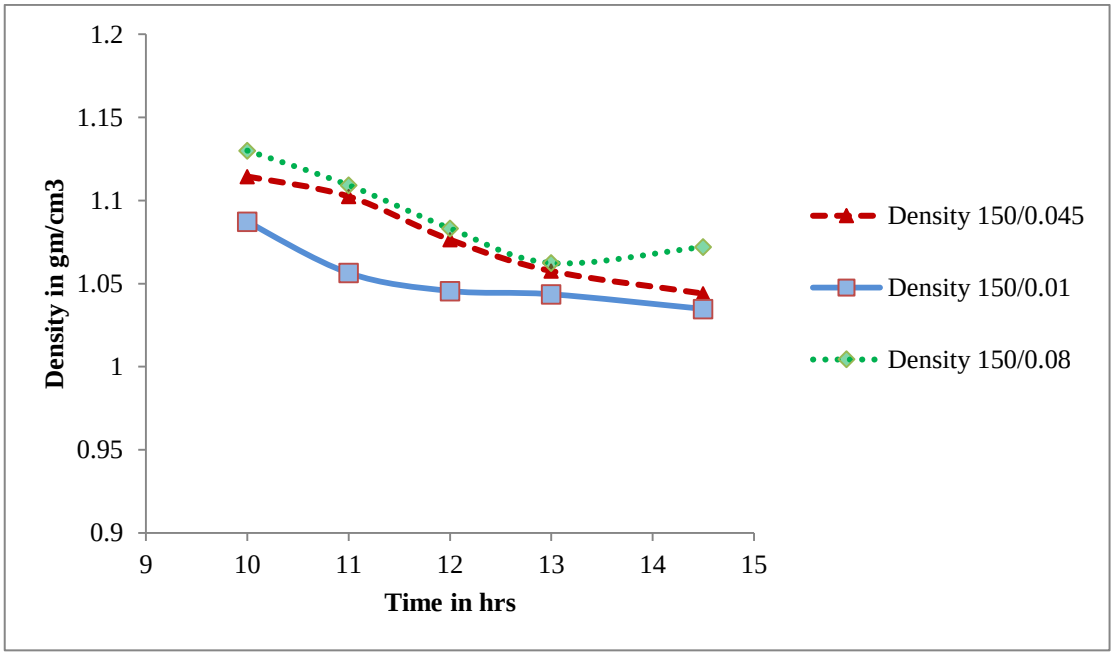

Figure4.24: Variation in Density of Al_2O_3-H_2O nanofluids of different volumetric concentration at 150LPH.

2) Variation in Density of Al_2O_3-H_2Onanofluids of different volumetric concentration (0.01%, 0.045%, 0.08%) at 200LPH.

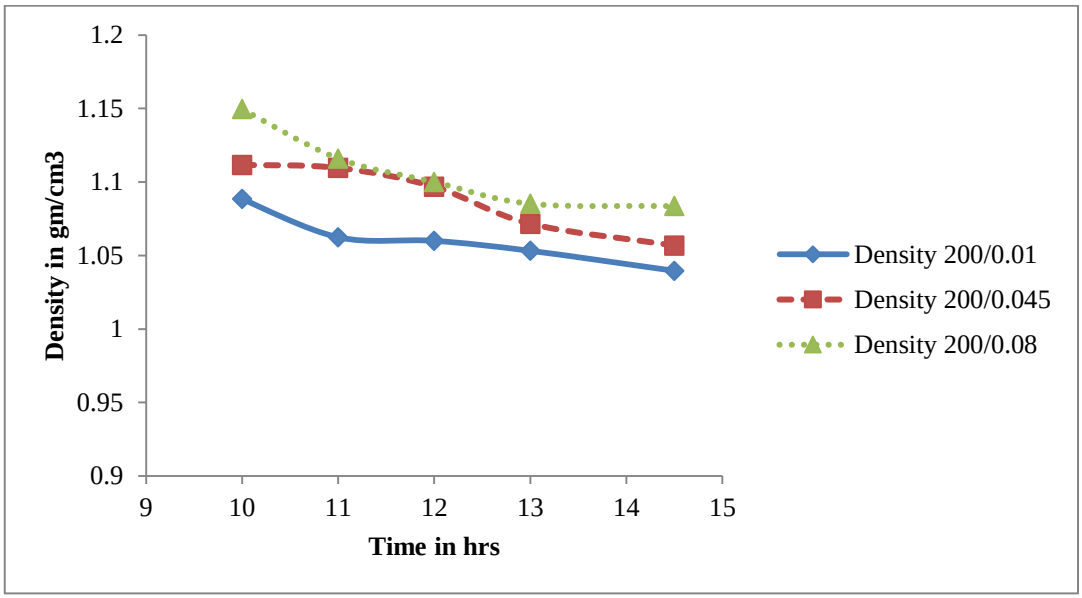

Figure4.25: Variation in Density of Al_2O_3-H_2O nanofluids of different volumetric concentration at 200LPH

3) Variation in Density of Al_2O_3-H_2Onanofluids of different volumetric concentration (0.01%, 0.045%, 0.08%) at 250LPH

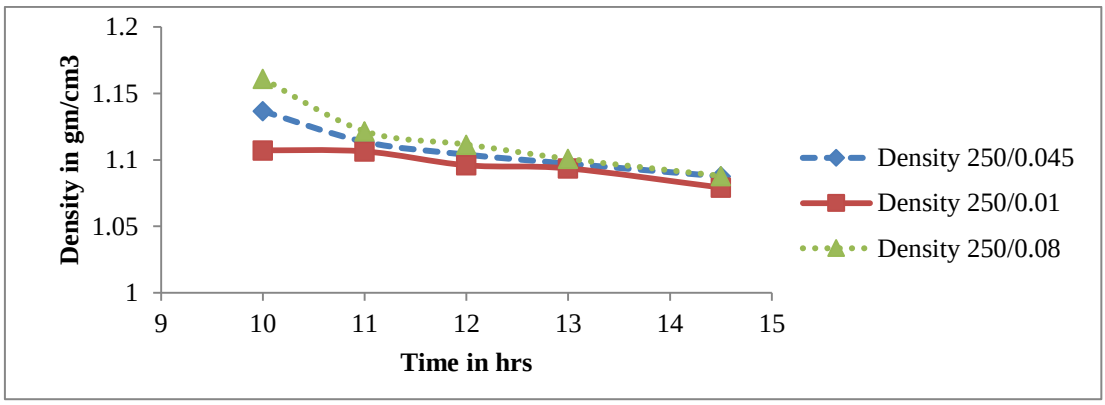

Figure4.26:Variation in Density of Al_2O_3-H_2O nanofluids of different volumetric concentration at 250LPH.

It is noticed from the Figure 4.24 to 4.26 that there is slight decrease (0.04 g/cm^3 to 0.075 g/cm^3) in density

4.6.2 Variation in ph

Graphs of variation in phAl_2O_3-H_2O nanofluids are observed with time of the day, at different mass flow rate (150LPH, 200LPH, 250LPH) and at different volumetric concentration (0.01%, 0.045%, 0.08%) are shown in Figure4.27 to 4.29.

4) Variation in ph of Al_2O_3-H_2Onanofluids of different volumetric concentration (0.01%, 0.045%, 0.08%) at150LPH mass flow rate.

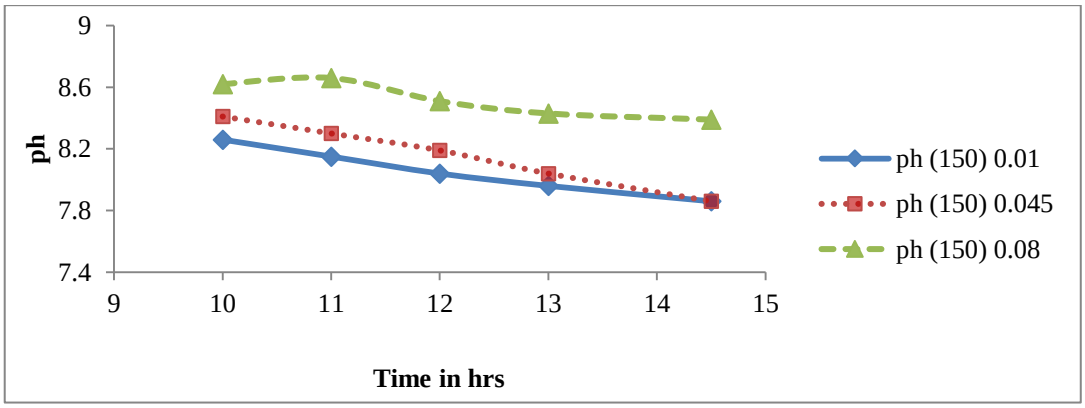

Figure4.27:Variation in ph of Al_2O_3-H_2Onanofluids of different volumetric concentration at 150LPH.

5) Variation in ph of Al_2O_3-H_2Onanofluids of different volumetric concentration (0.01%, 0.045%, 0.08%) at200LPH mass flow rate.

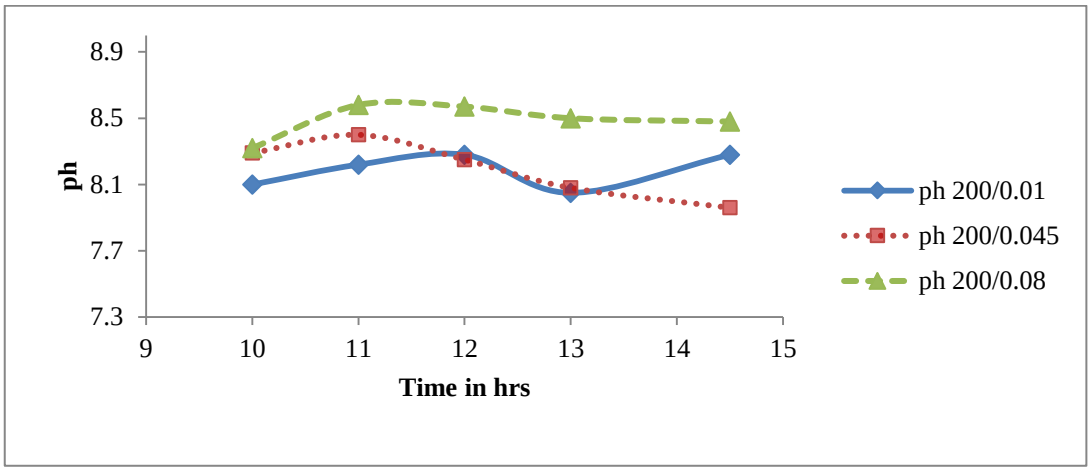

Figure4.28: Variation in ph of Al_2O_3-H_2Onanofluids of different volumetric concentration at 200LPH.

6) Variation in ph of Al_2O_3-H_2Onanofluids of different volumetric concentration (0.01%, 0.045%, 0.08%) at250LPH mass flow rate.

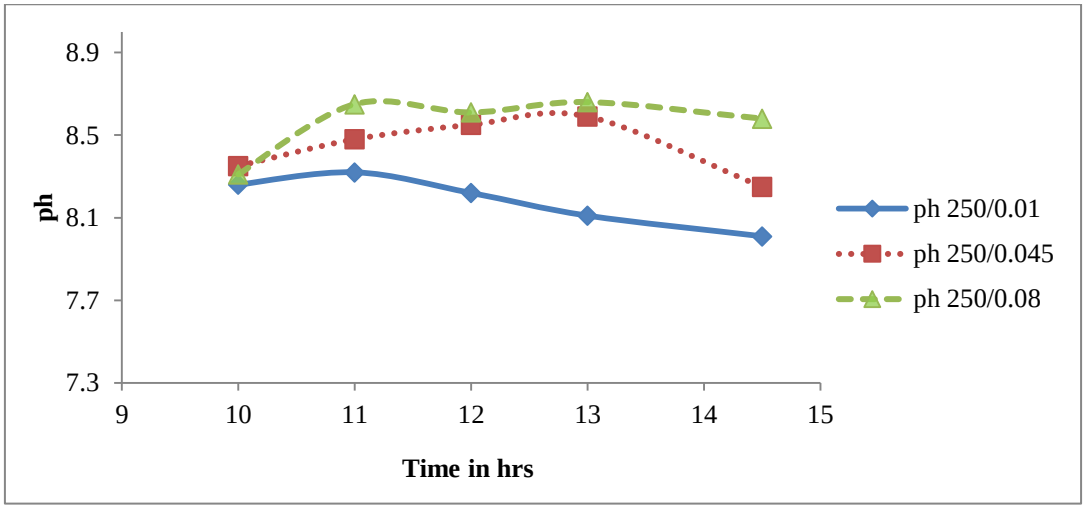

Figure4.29: Variation in ph of Al_2O_3-H_2Onanofluids of different volumetric concentration at 250LPH.

It is observed from the Figure 4.27 to 4.29 that ph value of Al_2O_3-H_2Onanofluid varies from 7 to 8.

4.6.3 Variation in Viscosity

Graphs of variation in Viscosity Al_2O_3-H_2O nanofluids are observed with time of the day, at 250LPH mass flow rate and at different volumetric concentration (0.01%, 0.045%, 0.08%) are shown in Figure4.30.

7) Variation in Viscosity of Al_2O_3-H_2O nanofluids of different volumetric concentration (0.01%, 0.045%, 0.08%) at 250LPH mass flow rate.

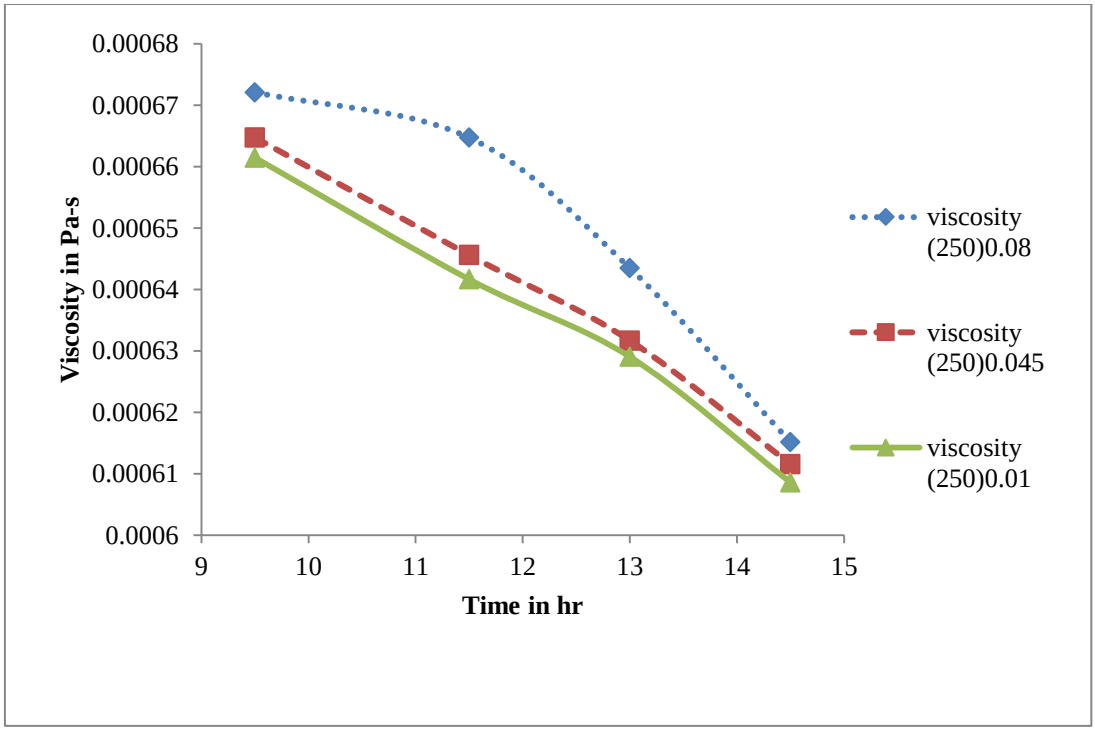

Figure4.30: Variation in Viscosity of Al_2O_3-H_2Onanofluids of different volumetric concentration at 250LPH.

From the above Figure it is observed that viscosity of Al_2O_3-H_2Onanofluid at 250 LPH with volumetric concentration of 0.01%, 0.045% and 0.08% decrease with time from 0.000672 Pa.s to 0.000608 Pa.s

4.6.4 Variation in Thermal Condutivity

Graphs of variation in the ratio Thermal Conductivity of Al_2O_3-H_2O nanofluids to the Thermal conductivity of base fluid, are observed with time of the day, at 200LPH mass flow rate and at different volumetric concentration (0.01%, 0.045%, 0.08%) are shown in Figure4.31.

8) Variation in Thermal Conductivity of Al_2O_3-H_2Onanofluids of different volumetric concentration (0.01%, 0.045%, 0.08%) at 250LPH mass flow rate.

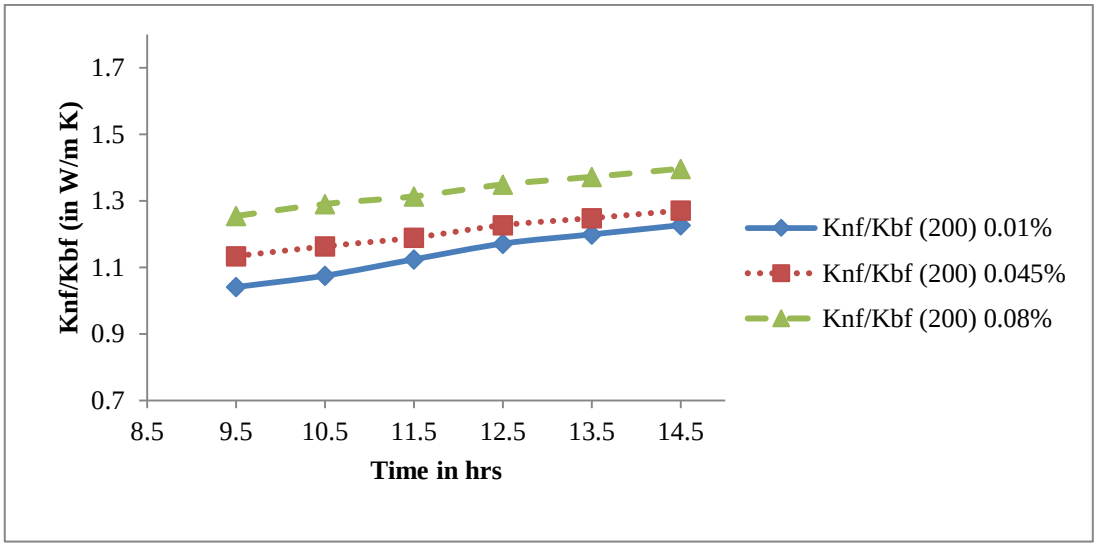

Figure4.31:Variation in Thermal Conductivity of Al_2O_3-H_2Onanofluids of different volumetric concentration at 250LPH

It is observed that ratio of thermal conductivity of Al_2O_3-H_2O nanofluids to the base fluid i.e. water increases with time of the day because as nanofluids are re-circulated in the solar heat collector its temperature increase so thermal conductivity of nanofluid increases, there is also increase in thermal conductivity of base fluid but very less in comparison to that of nanofluid, which leads to increase in the ratio of thermal conductivity of nanofluid to that of base fluid.

4.7Variation in Heat Gain with time of the day

Variation in the heat gain by the nanofluids of different volumetric concentration (0.01%, 0.045%, 0.08%) at different mass flow rates (150LPH, 200LPH, 250LPH) is observed in Figure4.32 to 4.34.

1) Variation in Heat gain by Al_2O_3-H_2O nanofluids of different volumetric concentration (0.01%, 0.045%, 0.08%) at 150LPH mass flow rate.

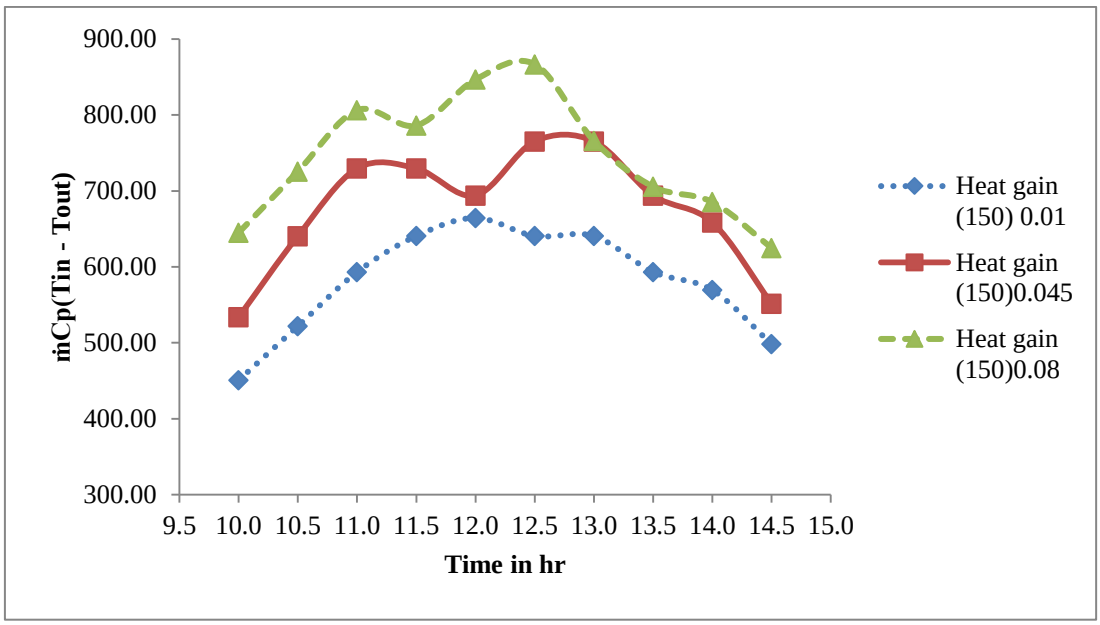

Figure4.32: Variation in Heat gain by Al_2O_3-H_2Onanofluids at 150LPH mass flow rate.

2) Variation in Heat gain by Al_2O_3-H_2Onanofluids of different volumetric concentration (0.01%, 0.045%, 0.08%) at 200LPH mass flow rate.

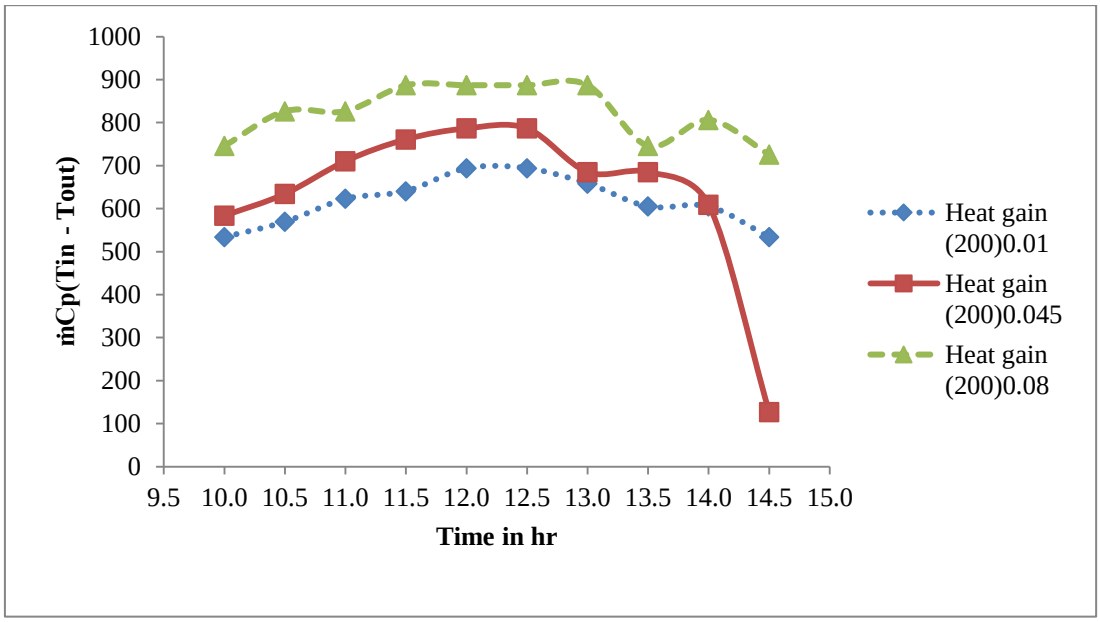

Figure4.33: Variation in Heat gain by Al_2O_3-H_2Onanofluids at 200LPH mass flow rate.

3) Variation in Heat gain by Al_2O_3-H_2Onanofluids of different volumetric concentration (0.01%, 0.045%, 0.08%) at 250LPH mass flow rate.

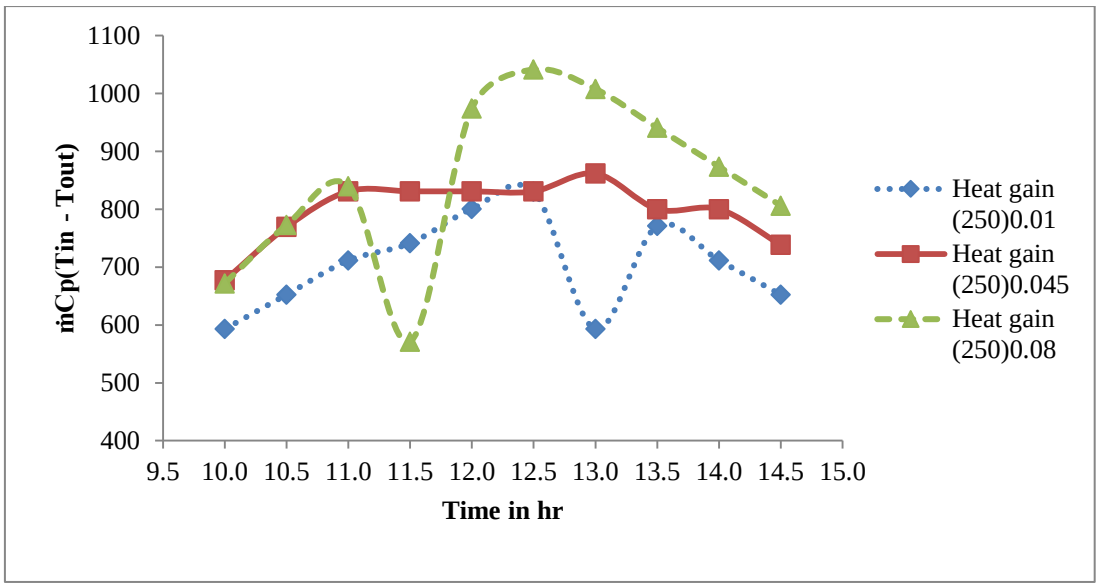

Figure4.34: Variation in Heat gain by Al_2O_3-H_2Onanofluids at 250LPH mass flow rate.

It is observed from the Figure 4.32, 4.33 and 4.34 that heat gain is maximum in between 11.00 am to 1.00 pm because solar intensity is maximum in this time period. Maximum heat gain by Al_2O_3-H_2Onanofluid is 1041 W at 250 LPH with 0.08% volumetric concentration.

Chapter 5

Conclusion and Future Scope

5.1 Conclusion

Experiments are performed with Al_2O_3-H_2O nanofluid of different volumetric concentration (0.01%, 0.045%, 0.08%) at different mass flow rates (150LPH, 200LPH, 250 LPH), Following are the conclusions

- It is observed that that a good solar intensity is received between 10.00 am to 3.00 pm.
- In convergent absorber tube instantaneous efficiency is slightly more (5% to 10%) than that of straight absorber tube, for Al_2O_3 – H_2O nanofluids.
- With increase in mass flow rate instantaneous efficiency increases.
- Viscosity of Al_2O_3-H_2O nanofluid decrease with time
- The ratio of thermal conductivity of Al_2O_3-H_2O nanofluids to the base fluid increases with temperature.
- Maximum heat gain by Al_2O_3-H_2O nanofluid is 1041 W at 250 LPH with 0.08% volumetric concentration.

5.2 Future Scope

A lot of more investigation can be done on nanofluid base parabolic heat collector. Following are the some future scope that can be done in this field

1) Proformence investigation can be done on cloudy days.
2) Investigation can be done with different nanofluid like TiO_2, Cuo, Zno etc. with different volumetric concentration can be used.
3) CFD analysis can be done on convergent absorber tube solar heat collector with different nanofluids.
4) Experimental and CFD investigation can be done with convergent divergent absorber tube.

References

1) D. John and B. William, Solar engineering and thermal process, fourth edition.
2) FarzadVeysi, TorajYousefi, EhsanShojaeizadeh, SirusZinadini, An experimental investigation on the effect of Al_2O_3-H_2O nanofluid on the efficiency of flat-plate solar collectors, Renewable Energy 39 (2012) 293-298.
3) www.renewableenergyhub.co.uk/thedifferent-types-of-solar-thermal-panel-collectors
4) I.M. Mahbubul, R. Saidur, M.A. Amalina, Latest developments on the viscosity of nanofluids, International Journal of Heat and Mass Transfer 55 (2012) 874-885.
5) J. Eastman, S. Choi, S. Li, W. Yu, L. Thompson, Anomalously increased effective thermal conductivities of ethylene glycol-based nanofluids containing copper nanoparticles, Appl. Phys. Lett. 78 (2001) 718–720.
6) H.-t. Zhu, Y.-s. Lin, Y.-s. Yin, A novel one-step chemical method for preparation of copper nanofluids, J. Colloid Interface Sci. 217 (2004) 100–103.
7) G. Paul, J. Philip, B. Raj, P.K. Das, I. Manna, Synthesis characterization and thermal property measurement of nano-Al95Zn05 dispersed nanofluid prepared by a two-step process, Int. J. Heat Mass Transfer 54 (2011) 3783–3788.
8) W. Yu, H. Xie, Y. Li, L. Chen, Experimental investigation on thermal conductivity and viscosity of aluminum nitride nanofluid, Particuology 9(2) (2011) 187–191.
9) D. Wen, Y. Ding, Formulation of nanofluids for natural convective heat transfer applications, Int. J. Heat Fluid Flow 26(6) (2005) 855–864.
10) E. Goharshadi, Y. Ding, M. Jorabchi, P. Nancarrow, Ultrasound-assisted greensynthesis of nanocrystallineZnO in the ionic liquid [hmim][NTf2], Ultrason. Sonochem 16 (2009) 120–123.
11) Jiang Y, Zou B, Dong J, Yao Y, An experimental investigation on a small-sized parabolic trough solar collector for water heating in cold areas, Applied Energy 163 (2016) 396-407.
12) M. K.S, K. G., V. R., and I. S., Parametric study of solar parabolic trough collector system, Asian J. Appl. Sci. 421 (2012) 1996–3343.
13) ErnaniFavale, GianpieroColangelo, Arturo de Risi, DomenicoLaforgia, Results of experimental investigations on the heat conductivity of nanofluids based on diathermic oil for high temperature applications, Applied Energy 97 (2012) 828–833.
14) ASHRAE Standard 86-93. Methods of testing to determine the thermal performance of solar collectors. 1986. Atlanta, GA, USA.

15) FarzadVeysi, TorajYousefi, EhsanShojaeizadeh, SirusZinadini, An experimental investigation on the effect of Al_2O_3-H_2O nanofluid on the efficiency of flat-plate solar collectors, Renewable Energy 39 (2012) 293-298.

16) FarzadVeysi, TorajYousefi, EhsanShojaeizadeh, SirusZinadini, An experimental investigation on the effect of MWCNT-H_2O nanofluid on the efficiency of flat-plate solar collectors, Experimental Thermal and Fluid Science 39 (2012) 207–212.

17) R. V. Padilla, A. Fontalvo, G. Demirkaya, A. Martinez, and A. G. Quiroga, Exergy analysis of parabolic trough solar receiver, *Appl. Therm. Eng.* 67,(2014)579–586.

18) M.H. Sajid, Z. Said, M.A. Alim, R. Saidur, N.A. Rahim, Experimental investigation of the thermo-physical properties of AL_2O_3-nanofluid and its effect on a flat plate solar collector, International Communications in Heat and Mass Transfer 48 (2013) 99–107.

19) E. Lüpfert, K.-J. Riffelmann, H. Price, F. Burkholder, and T. Moss, Experimental Analysis of Overall Thermal Properties of Parabolic Trough Receivers, *J. Sol. Energy Eng.* 130(2) (2008) 021007.

20) F. Nejati, K. Goudarzi, E. Shojaeizadeh, S.K. AsadiYousef-abad, Experimental study on the effect of pH variation of nanofluids on the thermal efficiency of a solar collector with helical tube, Experimental Thermal and Fluid Science 60 (2015) 20–27.

21) Larcher M, Rommel M, Bohren A, Frank E, Minder S, Characterization of a parabolic trough collector for process heat applications, Energy Procedia 57 (2014) 2804-2811.

22) GianpieroColangelo, ErnaniFavale, Arturo de Risi, DomenicoLaforgia, A new solution for reduced sedimentation flat panel solar thermal collector using nanofluids, Applied Energy 111 (2013) 80–93.

23) Hwang Y, Lee JK, Lee CH, Jung YM, Cheong SI, Lee CG, Stability and thermal conductivity characteristics of nanofluids, ThermochimActa 455 (2007) 70–4.

24) A. Ghadimi, R. Saidur, H.S.C. Metselaar, A review of nanofluid stability properties and characterization in stationary conditions, International Journal of Heat and Mass Transfer, 54 (2011) 4051–4068.

25) Anton J. M, Biencinto M, Zarza E, Diez L. E, Theoretical basis and experimental facility for parabolic trough collectors at high temperature using gas as heat transfer fluid, Applied Energy, 135 (2014) 373–381.

26) E. Bellos, C. Tzivanidis, K.A. Antonopoulos, G. Gkinis, Thermal enhancement of solar parabolic trough collectors by using nanofluids and converging-diverging absorber tube, Renewable Energy 94 (2016) 213-222.

27) Khullar V., Tyagi H., Phelan P.E., Otanicar T.P., Singh H., Taylor R.A., Solar Energy Harvesting Using Nanofluids Based Concentrating Solar Collector, Journal of Nanotechnology in Engineering and Medicine 3 (2012) 0310031- 0100319.
28) Hamilton RL, Crosser OK, Thermal conductivity of heterogeneous two component system, IEC Fundam 2 (1962) 187.
29) Zhang H, Liang H, You S, Comparison of different heat transfer models for parabolic trough solar collectors, Applied Energy 148 (2015)105-114.
30) Cheng Z. D, He Y. L, Wang K, Du B.C,Cui F.Q, A detailed parameter study on the comprehensive characteristics and performance of a parabolic trough solar collector system, Applied Thermal Engineering 63(2014) 278–289.

APPENDIX A

Table A.1 Solar intensity received in the month of April.

Time in hr	06.04.2017	14.04.2017	24.04.2017
9	313.098	373.065	405.381
10	455.256	500.233	547.201
11	524.847	605.008	650.712
12	569.817	667.487	686.759
13	572.702	644.748	667.658
14	145.464	570.009	595.615
15	295.819	434.416	493.377
16	177.501	288.818	341.342

Table A.2 Solar intensity received in the month of May.

Time in hr	02.05.2017	12.05.2017	22.05.2017
9	358.72	330.332	166.353
10	421.338	189.648	263.441
11	393.585	394.396	392.617
12	626.489	529.861	467.158
13	544.801	444.819	246.011
14	457.555	505.189	517.352
15	425.444	413.424	403.401
16	247.73	295.126	272.108

Table A.3 Solar intensity received in the month of June.

Time in hr	01.06.2017	05.06.2017	10.06.2017
9	346.504	316.61	458.224
10	470.212	432.846	622.022
11	557.94	498.346	730.935
12	596.43	543.751	778.933
13	454.968	535.569	797.998
14	542.788	471.532	683.01
15	419.841	377.04	517.065
16	292.45	256.751	348.859

APPENDIX B

Table A.4 Experimental data for 0.01% Al_2O_3-H_2O nanofluid as working fluid at 150 LPH (30/05/2017)

Time in hrs	Inlet temp (°C)	Outlet temp (°C)	Global solar Intensity	Heat gain (150) 0.01 (J)	ηi convergent (150) 0.01	ηt convergent (150) 0.01
10	38.2	40.1	473.125	450.84	42.7397	46.0787
10.5	45.9	48.1	524.902	522.03	44.6065	48.0913
11	53.3	55.8	564.11	593.21	47.166	50.8509
11.5	60.6	63.3	594.232	640.67	48.3572	52.1351
12	67.1	69.9	596.802	664.40	49.9322	53.8332
12.5	73.2	75.9	608.062	640.67	47.2574	50.9493
13	78	80.7	586.733	640.67	48.9753	52.8014
13.5	81.5	84	554.242	593.21	48.0059	51.7563
14	82.5	84.9	514.029	569.48	49.691	53.5731
14.5	81.2	83.3	465.728	498.30	47.9889	51.738

Time in hrs	ph (150) 0.01	Density 150/0.01
10	8.41	1.0872
11	8.3	1.0564
12	8.19	1.0456
13	8.04	1.0436
14.5	7.86	1.0348

Table A.5 Experimental data for 0.045% Al_2O_3-H_2O nanofluid as working fluid at 150 LPH (24/05/2017)

Time in hrs	Inlet temp (°C)	Outlet temp (°C)	Global solar Intensity (W/m^2)	Heat gain (150)0.045 (J)	ηi convergent (150)0.045	ηt convergent (150)0.045
10	36.1	39.1	498.168	533.8857919	48.06794329	51.82323466
10.5	43.6	47.2	541.59	640.6629503	53.05686577	57.20191497
11	50	54.1	588.44	729.6439156	55.61494239	59.95984043
11.5	57.5	61.6	586.895	729.6439156	55.76134788	60.1176838
12	63	67.1	576.267	729.6439156	56.78975169	61.22643131
12.5	68.8	73.1	595.062	765.2363018	57.6787226	62.18485276
13	74	78.3	604.435	765.2363018	56.78431093	61.22056549
13.5	79.2	83.1	599.514	694.0515295	51.92485749	55.98146894
14	83.2	86.9	555.786	658.4591434	53.13781305	57.28918622
14.5	81	84.1	489.075	551.681985	50.59367952	54.54629315

Time in hrs	ph (150) 0.045	Density 150/0.045
10	8.26	1.1144
11	8.15	1.1024
12	8.04	1.0764
13	7.96	1.0576
14.5	7.86	1.044

Table A.6 Experimental data for 0.08% Al_2O_3-H_2O nanofluid as working fluid at 150 LPH (02/06/2017)

Time in hrs	Inlet temp (^oC)	Outlet temp (^oC)	Global solar Intensity (W/m^2)	Heat gain (150)0.08 (J)	η_i convergent (150)0.08	η_t convergent (150)0.08
10	40.6	43.8	480.716	645.087	60.1884	64.8906
10.5	49.5	53.1	518.096	725.723	62.8266	67.7349
11	57.1	61.1	565.751	806.359	63.9272	68.9215
11.5	63.4	67.3	546.068	786.2	64.5756	69.6206
12	69.9	74.1	578.781	846.677	65.6125	70.7385
12.5	76	80.3	609.355	866.836	63.8042	68.7888
13	81.9	85.7	568.377	766.041	60.4503	65.173
13.5	80.9	84.4	513.954	705.564	61.5736	66.384
14	79.5	82.9	496.815	685.405	61.8778	66.712
14.5	81	84.1	461.032	624.929	60.797	65.5467

Time in hrs	ph (150) 0.08	Density 150/0.08
10	8.62	1.13
11	8.66	1.1092
12	8.51	1.0832
13	8.43	1.0624
14.5	8.39	1.072

APPENDIX C

Table A.7 Experimental data for 0.01% Al_2O_3-H_2O nanofluid as working fluid at 200 LPH (26/05/2017)

Time (hrs)	Inlet temp (°C)	Outlet temp (°C)	Global solar Intensity (W/m^2)	Heat gain (200)0.01 (J)	η_i convergent (200)0.01	η_t convergent (200)0.01
10	38.9	41.9	450.2019	533.8858	53.18922	57.34461
10.5	47.3	50.5	493.1039	569.4782	51.79899	55.84576
11	55.1	58.6	521.1867	622.8668	53.60243	57.7901
11.5	62.3	65.9	538.7	640.663	53.3415	57.50878
12	68.4	72.3	554.1121	694.0515	56.17934	60.56833
12.5	73.2	77.1	554.4789	694.0515	56.14218	60.52827
13	78.8	82.5	549.9686	658.4591	53.6999	57.89519
13.5	81.5	84.9	528.5057	605.0706	51.34982	55.36151
14	85.8	89.2	513.9395	605.0706	52.80519	56.93058
14.5	82.3	85.3	454.8537	533.8858	52.64525	56.75815

Time in hrs	ph 200/0.01	Density 200/0.01	Time in hr	Knf/Kbf (200) 0.01%
10	8.1	1.0884	**9.5**	1.04078
11	8.22	1.0624	**10.5**	1.07504
12	8.28	1.06	**11.5**	1.12398
13	8.05	1.0532	**12.5**	1.17129
14.5	8.28	1.0396	**13.5**	1.19902
			14.5	1.22675

Table A.8 Experimental data for 0.045% Al_2O_3-H_2O nanofluid as working fluid at 200 LPH (26/05/2017)

Time in hrs	Inlet temp (°C)	Outlet temp (°C)	Global solar Intensity (W/m^2)	Heat gain (200)0.045 (J)	η_i convergent (200)0.045	η_t convergent (200)0.045
10	41	43.3	435.8482	583.5674	60.0535	64.74516
10.5	48.6	51.1	474.8877	634.3124	59.90938	64.58978
11	55.6	58.4	515.6635	710.4298	61.79273	66.62027
11.5	62.5	65.5	541.9475	761.1748	62.99554	67.91705
12	69.1	72.2	534.4005	786.5473	66.01468	71.17206
12.5	73.9	77	540.4129	786.5473	65.28023	70.38023
13	75.1	77.8	496.088	685.0573	61.93709	66.7759
13.5	78.5	81.2	519.6966	685.0573	59.12344	63.74243
14	81	83.4	461.8718	608.9399	59.13377	63.75357
14.5	72.8	73.3	98.87593	126.8625	57.54733	62.04319

Time in hrs	ph 200/0.045	Density 200/0.045	Time in hr	Knf/Kbf (200) 0.045%
10	8.29	1.1116	**9.5**	1.13377
11	8.4	1.1096	**10.5**	1.16313
12	8.25	1.0968	**11.5**	1.18923
13	8.08	1.0716	**12.5**	1.22675
14.5	7.96	1.0568	**13.5**	1.24796
			14.5	1.2708

Table A.9 Experimental data for 0.08% Al_2O_3-H_2O nanofluid as working fluid at 200 LPH (09/06/2017)

Time in hrs	Inlet temp (ºC)	Outlet temp (ºC)	Global solar Intensity (W/m^2)	Heat gain (200)0.08 (J)	η_i convergent (200)0.08	η_t convergent (200)0.08
10	39.5	43.2	484.6725	745.8824	69.02471	74.41724
10.5	47.6	51.7	529.6772	826.5184	69.98803	75.45582
11	55.5	59.6	529.4646	826.5184	70.01614	75.48612
11.5	62.8	67.2	578.3082	886.9953	68.79305	74.16748
12	69.3	73.7	562.4402	886.9953	70.73389	76.25995
12.5	74.9	79.3	592.3885	886.9953	67.15793	72.40462
13	78.4	82.8	592.1332	886.9953	67.18688	72.43583
13.5	79.3	83	507.5083	745.8824	65.91887	71.06876
14	80.2	84.2	540.5648	806.3594	66.90575	72.13274
14.5	80.3	83.9	479.1246	725.7234	67.93682	73.24436

Time in hrs	ph 200/0.08	Density 200/0.08	Time in hr	Knf/Kbf (200) 0.08%
10	8.32	1.1496	**9.5**	1.25449
11	8.58	1.116	**10.5**	1.29038
12	8.57	1.1	**11.5**	1.31321
13	8.5	1.0852	**12.5**	1.3491
14.5	8.48	1.0836	**13.5**	1.37194
			14.5	1.39641

APPENDIX D

Table A.10 Experimental data for 0.01% Al_2O_3-H_2O nanofluid as working fluid at 250 LPH (01/06/2017)

Time in hrs	Inlet temp (ºC)	Outlet temp (ºC)	Global solar Intensity (W/m^2)	Heat gain (250)0.01 (J)	η_i convergent (250)0.01	η_t convergent (250)0.01
10	41.2	43.2	470.212	593.079	56.572	60.9917
10.5	48.5	50.7	519.471	652.387	56.3283	60.7289
11	54.2	56.6	557.94	711.695	57.2122	61.6819
11.5	59.9	62.4	568.149	741.349	58.5252	63.0975
12	65.1	67.8	596.43	800.657	60.2101	64.914
12.5	69	71.8	616.746	830.311	60.3833	65.1007
13	73.2	75.2	454.968	593.079	58.4674	63.0352
13.5	76.9	79.5	594.794	771.003	58.1396	62.6817
14	81.1	83.5	542.788	711.695	58.8093	63.4038
14.5	80	82.2	493.285	652.387	59.3185	63.9527

Time in hrs	ph 250/0.01	Density 250/0.01	Time in hrs	viscosity (250)0.01
10	8.26	1.1072	**9.5**	0.00066
11	8.32	1.1064	**11.5**	0.00064
12	8.22	1.096	**13**	0.00063
13	8.11	1.0936	**14.5**	0.00061
14.5	8.01	1.0792		

Table A.11 Experimental data for 0.045% Al_2O_3-H_2O nanofluid as working fluid at 250 LPH (14/06/2017)

Time in hrs	Inlet temp (ºC)	Outlet temp (ºC)	Global solar Intensity (W/m^2)	Heat gain (250)0.045	η_i convergent (250)0.045	η_t convergent (250)0.045
10	40.6	42.8	450.489	677.076	67.4118	72.6783
10.5	47.5	50	502.375	769.405	68.6925	74.0591
11	54.1	56.8	541.137	830.957	68.8737	74.2545
11.5	59.9	62.6	553.959	830.957	67.2796	72.5358
12	66.2	68.9	523.103	830.957	71.2482	76.8145
12.5	71	73.7	535.831	830.957	69.5558	74.9898
13	75.9	78.7	554.772	861.734	69.6693	75.1122
13.5	80	82.6	539.763	800.181	66.4917	71.6864
14	83.1	85.7	501.784	800.181	71.5244	77.1122
14.5	83.8	86.2	484.672	738.629	68.3536	73.6937

Time in hrs	ph 250/0.045	Density 250/0.045	Time in hrs	viscosity (250)0.045
10	8.35	1.1368	**9.5**	0.00066
11	8.48	1.1136	**11.5**	0.00065
12	8.55	1.104	**13**	0.00063
13	8.59	1.0972	**14.5**	0.00061
14.5	8.25	1.0876		

Table A.12 Experimental data for 0.08% Al_2O_3-H_2O nanofluid as working fluid at 250 LPH (15/06/2017)

Time in hrs	Inlet temp (^oC)	Outlet temp (^oC)	Global solar Intensity (W/m^2)	Heat gain (250)0.08	η_i convergent (250)0.08	η_t convergent (250)0.08
10	42.3	44.3	425.584	671.958	70.8173	76.3498
10.5	49.4	51.7	472.282	772.752	73.3874	79.1208
11	54.1	56.6	510.217	839.948	73.838	79.6066
11.5	59.4	61.1	339.247	571.165	75.5142	81.4137
12	63	65.9	573.25	974.34	76.2341	82.1898
12.5	66.8	69.9	598.281	1041.54	78.082	84.1822
13	71.1	74.1	573.811	1007.94	78.7857	84.9408
13.5	75.2	78	556.277	940.742	75.8511	81.777
14	79.2	81.8	513.139	873.546	76.3542	82.3194
14.5	82.5	84.9	470.314	806.35	76.8985	82.9062

Time in hrs	ph 250/0.08	Density 250/0.08	Time in hrs	viscosity (250)0.08
10	8.31	1.1612	**9.5**	0.00067
11	8.65	1.1216	**11.5**	0.00066
12	8.61	1.1116	**13**	0.00064
13	8.66	1.1008	**14.5**	0.00062
14.5	8.58	1.088		

APPENDIX E

Table A.13 Experimental data for H_2O as working fluid at 150 LPH (13/06/2017)

Time in hrs	Inlet temp (°C)	Outlet temp (°C)	Global solar Intensity (W/m^2)	ηi Water 150	ηt Water 150
10:00	40.2	42.1	592.497	24.73898945	26.6717144
10:30	48.1	50.3	662.551	25.61638708	27.61765842
11:00	54.5	56.9	701.34	26.39958761	28.46204622
11:30	60.3	62.9	755.027	26.56595152	28.64140725
12:00	65.5	68.2	774.682	26.88777153	28.98836934
12:30	70	72.7	769.541	27.06739813	29.1820292
1:00	74.2	76.7	758.381	25.43121297	27.41801765
1:30	78.7	81.2	722.889	26.67982045	28.76417215
2:00	79	81.4	679.662	27.24160947	29.36985074
2:30	79.6	81.7	620.122	26.12502206	28.16603033

Table A.14 Experimental data for H_2O as working fluid at 200 LPH (03/06/2017)

Time in hrs	Inlet temp (°C)	Outlet temp (°C)	Global solar Intensity (W/m^2)	ηi Water 200	ηt Water 200
10:00	35.2	36.5	480.7161	27.81684658	29.99002805
10:30	42.6	44	518.0957	27.79529414	29.96679183
11:00	50.2	51.8	565.7513	29.090266	31.36293292
11:30	57.6	59.2	546.0685	30.13881213	32.49339635
12:00	66.8	68.6	578.7806	31.98982135	34.48901503
12:30	75.2	77.1	609.3554	32.07274784	34.57842012
1:00	75.9	77.6	568.3766	30.7656422	33.16919731
1:30	74.7	76.3	513.9545	32.02200775	34.52371597
2:00	75.3	76.9	496.8154	33.12669908	35.71471093
2:30	75.6	77.1	461.0318	33.46675359	36.08133208

Table A.15 Experimental data for H_2O as working fluid at 250 LPH (12/06/2017)

Time in hrs	Inlet temp (°C)	Outlet temp (°C)	Global solar Intensity (W/m^2)	ηi Water 250	ηt Water 250
10:00	36	37.4	494.3892242	36.40961154	39.25409979
10:30	43.9	45.4	545.564662	35.35102683	38.11281351
11:00	63.3	64.9	564.0130323	36.47437422	39.32392203
11:30	68	69.7	596.966924	36.61471503	39.47522691
12:00	71.8	73.7	619.1096096	39.45872625	42.54142552
12:30	75	76.9	616.9798574	39.59493379	42.68827423
1:00	78	79.8	603.2618577	38.36397894	41.36115146
1:30	80.2	81.9	571.0138908	38.2788828	41.26940721
2:00	80	81.7	551.3033897	39.64745041	42.74489369
2:30	78.5	80	483.3309818	39.9028238	43.02021804